# Surveying for geotechnical engineers

Author: Prof. Dr.-Ing. habil. Heinz Konietzky
(TU Bergakademie Freiberg, Geotechnical Institute)

## 1  Introduction

Surveying (land surveying, mining surveying etc.) or more generally spoken geodesy is an engineering discipline which delivers valuable data for engineers dealing with geotechnical or rock mechanical problems. With quite different techniques surveyors determine or monitor ground movements and deduce related values like subsidence, heave, inclinations, tilting, strains etc. They also deliver digital elevation models (DEM) useful for the setup of numerical models for more detailed rock mechanical stability and deformation analysis. The surveying can vary from micro-scale to macro-scale, depending on the task and the used technique, resolution and size of the considered objects. Surveying data are important for geoengineers in several directions, they can be used for instance for:

- Monitoring of surface movements for risk evaluation and early warning systems
- Evaluation of functionality of geotechnical support measures
- Validation of numerical simulation results
- Set-up of DEMs
- Geotechnical backanalysis
- Research in respect to unsolved geotechnical phenomena
- Preservation of evidence
- Documentation of archaeological sites
- etc. …

## 2   Classification of surveying techniques

According to the object, surveying can be classified by the following types:

- Engineering Surveying (roads, railways, reservoirs etc.)
- Military Surveying
- Mine Surveying
- Geological Surveying
- Marine Surveying
- Archaeological Surveying

In general, one can distinguish between geodetic and plane surveying. Geodetic surveying is performed on an ellipsoid, representing in first approximation the earth, to make precise measurements over large areas and distances, respectively. Plane surveys are performed on an assumed plane to compute horizontal positions (earth is approximated by a flat plane, curvature can be corrected). Fig. 2.1 illustrates the five basic types of surveying. According to the used instruments and methods, respectively, surveying can be classified as follows (see also Fig. 2.2):

- Chain surveying
- Compass surveying
- Theodolite surveying (measuring horizontal and vertical angles)
- Traverse surveying
- Triangulation surveying
- Tachometric surveying
- Plane table surveying
- Photogrammetric surveying
- Laser scanning based surveying
- Aerial surveying
- Satellite surveying (remote sensing)

Surveying for geotechnical engineers

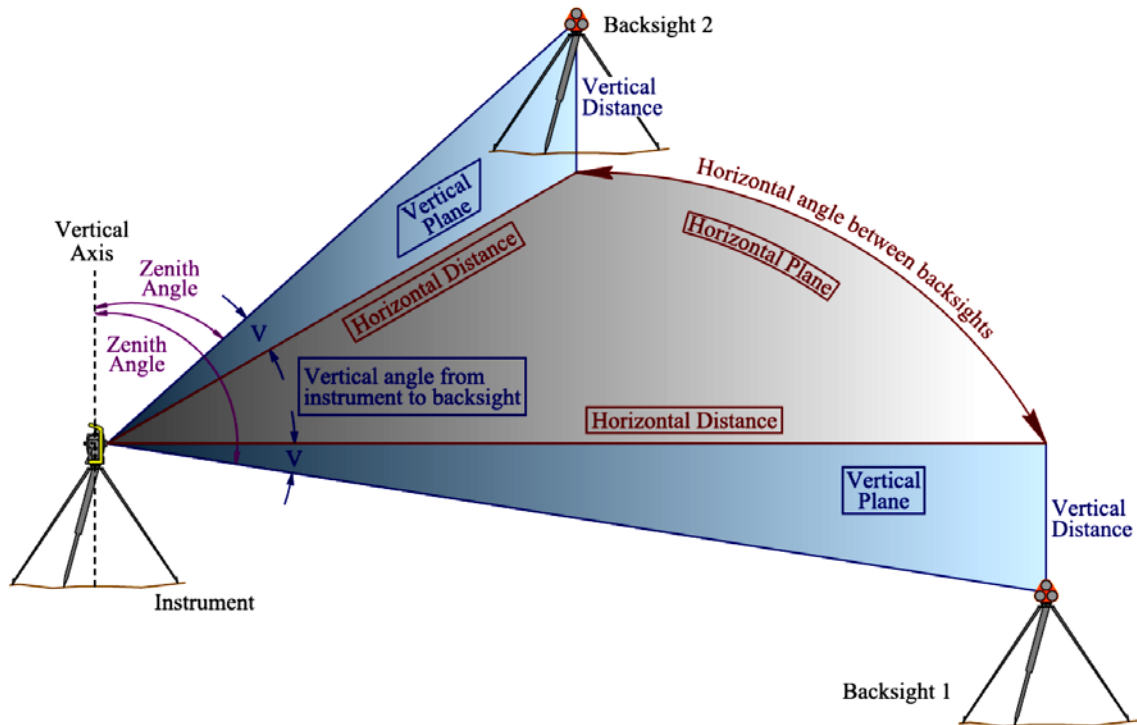Only for private and internal use!                                    Updated: 05 March 2021

Fig. 2.1: Five common types of survey measurements: horizontal distances and angles, vertical distances and angles, slope distances (Wyoming, 2013).
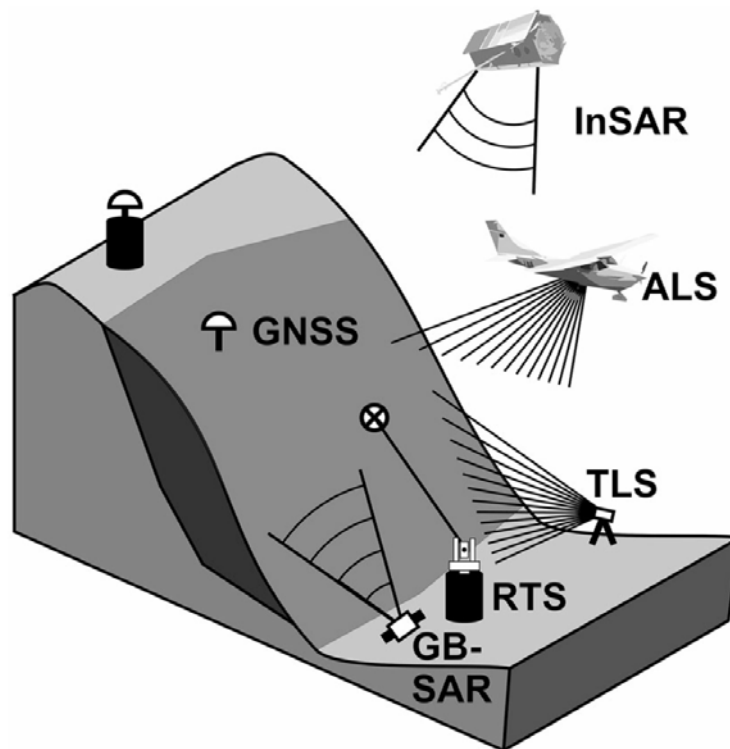
Fig. 2.2: Illustration of different monitoring methods: ALS = Airborne laser scanning, TLS = Terrestric laser scanning, RTS = Robotic Total Station, InSAR = Interferometric Synthetic Aperture Radar, GNSS = Global Navigation Satellite System, GBSAR = Ground Based Synthetic Aperture Radar (Lienhart, 2017)

Tab. 2.1: Characterization of typical survey techniques (Ogundare, 2016)

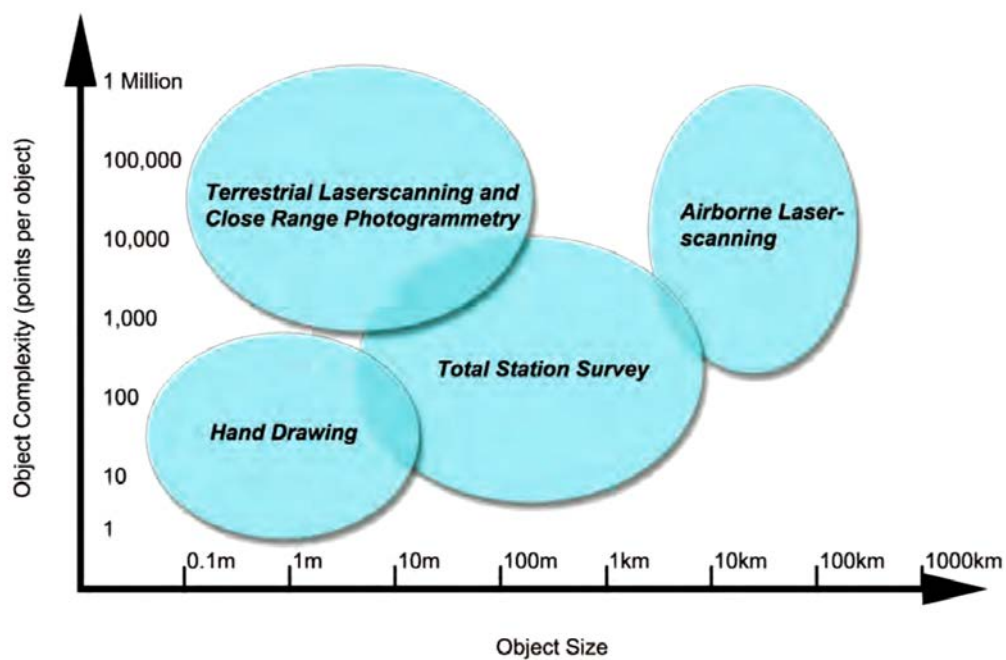| Survey Techniques | Typical Observables |
|---|---|
| Differential leveling | Elevation (leveled height) differences between sections |
| Trigonometric leveling | Zenith (or vertical) angles, slope (or horizontal) distances, heights of instruments, heights of targets or staff readings, and horizontal directions (or angles) |
| Traverse | Horizontal directions (or angles), horizontal (or slope) distances, zenith (or vertical) angles, and bearings |
| Triangulation | Horizontal directions (or angles), zenith (or vertical) angles, baseline distances, and bearings |
| Trilateration | Horizontal (or slope) distances, zenith angles, and bearings |
| Gyro station/gyrotheodolite measurements | Astronomic azimuths (or bearings) |
| GPS surveys | Baseline vectors (coordinate differences of baselines) and ellipsoidal heights |
| Gravimetric leveling | Relative gravity values |
| Conventional photogrammetry | Photo coordinates of points $(x, y)$; coordinates of fiducial center $(x_0, y_0)$ of photo; focal length of camera $(f)$; orientation of photo in space (if measured using gyro or inertia navigation system), such as $\Omega_0, \Phi_0, K_0$; and translations $(X_0, Y_0, Z_0)$ if measured using GPS |
| Close-range photogrammetry and remote sensing | Distances in laser altimeters; phase shifts and intensity values of returned radar energy in interferometric synthetic aperture radar (InSAR); and the $x, y, z$ coordinates (or the vertical angles, horizontal angles, and slope distances) in light detection and ranging (LiDAR) scanning systems |



Fig. 2.3: Typical application scales for different surveying methods (Opitz, 2013)

Surveying for geotechnical engineers

Only for private and internal use!                    Updated: 05 March 2021

Tab. 2.2: Main differences between InSAR and GB-InSAR (Ogundare, 2016)

|  | Space-Borne InSAR | GB-InSAR |
|---|---|---|
| 1. Rate of image acquisition | Several days or weeks | Few minutes (as often as 5 or 10 min) |
| 2. Working range/altitude | Several hundred kilometers away (about 800 km in altitude) | Few kilometers away (up to 4 km) in line-of-sight distance of the area being mapped |
| 3. How synthetic aperture of radar is obtained | Obtained by the antenna moving round an orbit | Obtained by an antenna traveling back and forth on a mechanical rail of about 2–3 m long |
| 4. Ground horizontal spatial resolution size | Depends on satellite, radar instrument, and look angle of radar; ranges from 3 to 30 m (TerraSAR-X has a variable resolution, typically 3 m by 3 m) | Few decimeters to several meters depending on the equipment and the monitoring distance (a typical commercial equipment has a resolution of about 0.5 by 4 m at 1 km) |

The selection of the appropriate surveying technique depends on serval factors and in the most cases it's a trade-off. Sometimes a combination of several techniques is recommended. The most important factors are:

- Required accuracy
- Costs
- Availability
- Robustness
- Distance between device and object
- Access to object
- Size of object
- Duration of monitoring

Surveying for geotechnical engineers

Only for private and internal use! Updated: 05 March 2021

# 3 Selected popular surveying techniques in geoengineering

## 3.1 Total station measurements

Typical components of a total station are:

- Total station measuring unit
- Reflectors
- Tripod
- Tribrach
- GNSS poles
- Levelling bars
- Micro-processor incl. data acquisition system

Total stations allow to measure distances, horizontal and vertical angles as well as elevations in topographic areas. Measuring distances can reach up to a few kilometres, but they are typical in the range of a few 100 m. Data management is done by a micro-processor.



Fig. 3.1.1: Total station with levelling bars and reflector (Leica geosystems, company material)

## 3.2 Satellite / aerial based measurements

Different satellite systems exist, like the Russian system 'GLONASS', the Chinese system 'BeiDou', the US system 'NAVSTAR GPS' or the European system 'Galileo'. If several systems are used the term GNSS (Global Navigation Satellite System) is used. Satellite based measuring systems need a receiver and contact with several satellites (see Fig. 3.2.1). Horizontal accuracy is in the range of millimetres, while vertical accuracy is in the order of centimetres. In case of further detailed processing the vertical accuracy can be further improved towards millimetres. Two types of GNSS surveying can be distinguished: static and dynamic; and two methods can be distinguished: relative positioning and absolute positioning (see Fig. 3.2.2). Accuracy of the static method is higher than those of the dynamic method.

Static surveying uses two or more stationary (fixed) receivers. The operation time of the receivers is called occupation. The longer the occupation time, the better the resolution. Dynamic surveys obtain one fixed station and several others moving around.

Surveying for geotechnical engineers

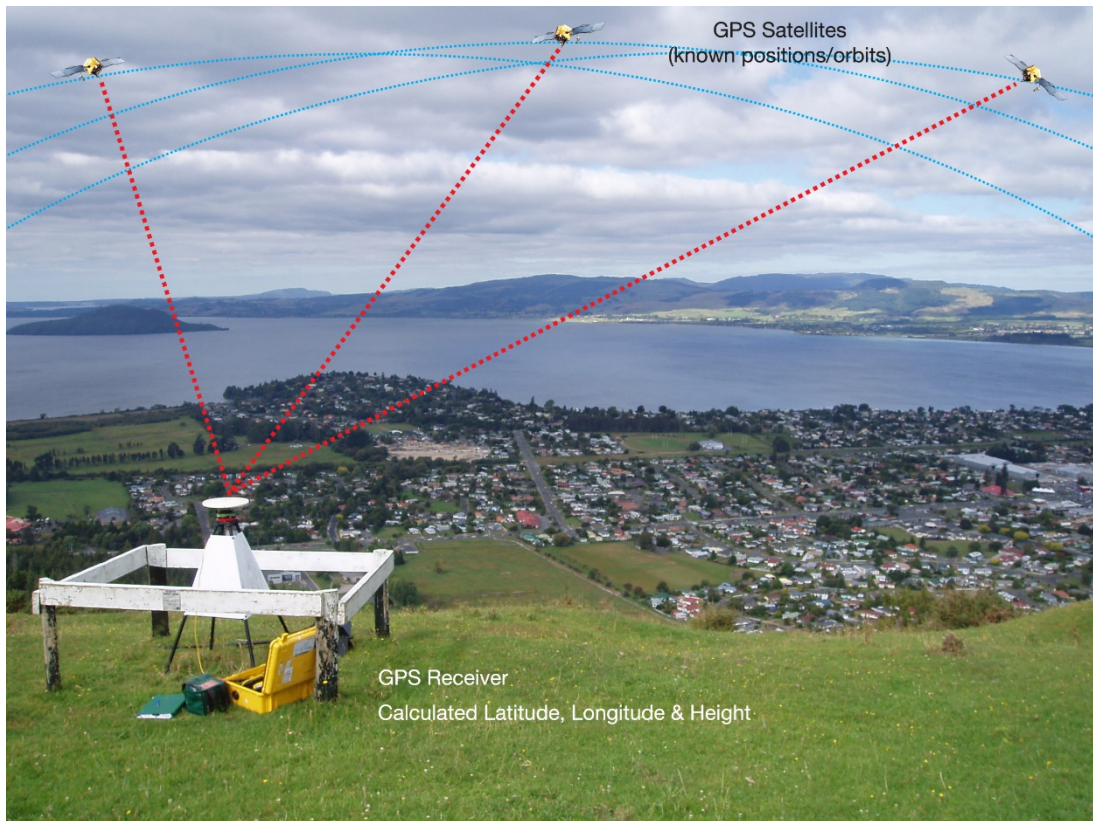Only for private and internal use!                    Updated: 05 March 2021

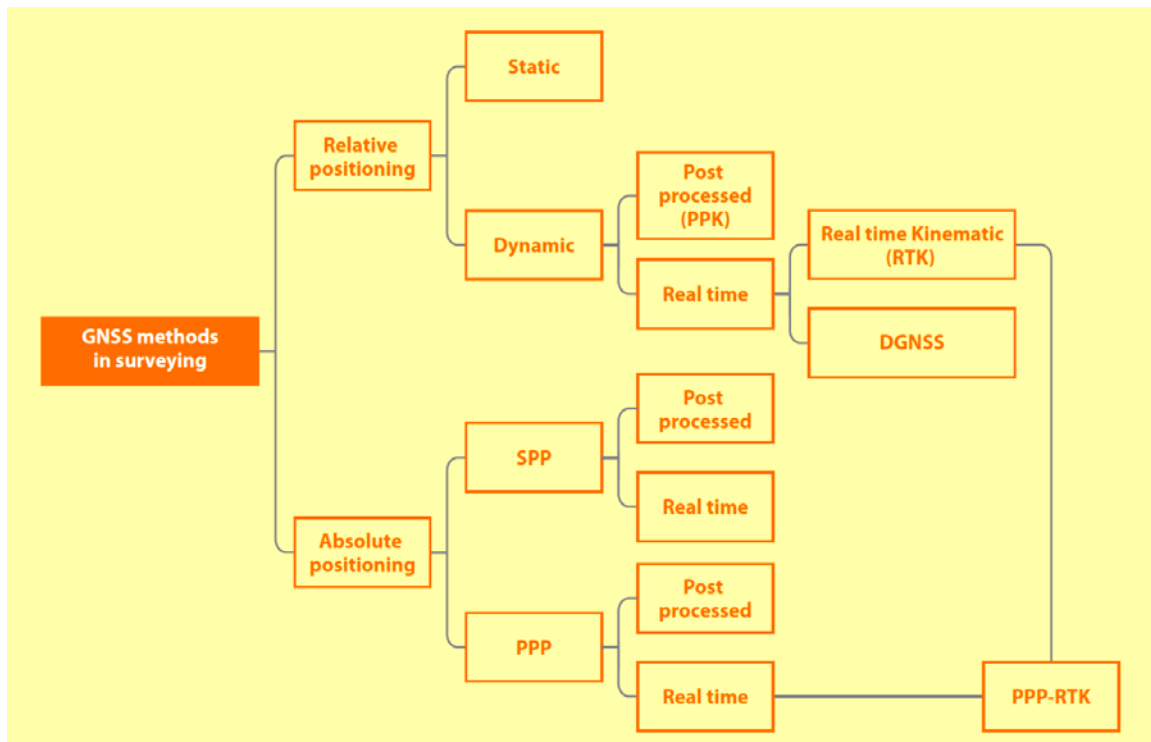Fig. 3.2.1: Illustration of the operation of a GNSS system (here: GPS)



Fig. 3.2.2: Classification of GNSS (PPP = Precise Point Positioning; SPP = Single Point Positioning;
DGNSS = Differential GNSS; RTK = Real Time Kinematic, PPK = Post Processing Kinematics)

Unmanned aerial systems (UAVs) are becoming more and more popular due to flexibility, low costs and fast data acquisition (see Tab. 3.2.1 and 3.2.2). An UAV system (see Fig. 3.2.2) consists of the following parts:

- Airframe incl. navigation system (GNSS), inertial navigation system, power system, flight control system and measuring unit

- Ground control system

- Communication system

The measuring unit can comprise:

- Digital photo cameras (images or videos; photogrammetry see Fig. 3.2.3)

- Thermal cameras based on infrared radiation measurements

- Multispectral cameras (observation of non-visible light of specific spectra)

- LiDAR (Light detection and ranging)

Tab. 3.2.1: Comparison of different types of UAVs: 1 = low, 5 = high (Gordian et al., 2020)

| UAV | Range | Duration | Wind influence | Operability |
|---|---|---|---|---|
| Balloon | 1 | 4 | 4 | 2 |
| Airship | 3 | 3 | 4 | 3 |
| Kite | 2 | 2 | 4 | 2 |
| Fixed wings | 5 | 5 | 2 | 4 |
| Helicopter (mini) | 4 | 4 | 3 | 5 |
| Multirotor (with 4–8 propellers) | 4 | 3 | 2 | 5 |

Tab. 3.2.2: Advantages of UAV surveying (Gordian et al., 2020)

| Requirement | Purpose | UAV photogrammetry advantage |
|---|---|---|
| Safety assessment | Communication with local authorities, emergency services, and public | Rapid deployment and processing |
| Reconnaissance | Fieldwork planning, contextual mapping, and planning of ground investigation. Disaster response | Rapid deployment and processing, and flexibility of scale |
| 3D modeling | Responsive visual assessment, rapid geomorphological assessment and zoning of landslides, monitoring rates of erosion, design of ground investigations, design of TLS survey, and slope stability analysis | Speed, repeatability, compatibility with other survey methods, flexibility of scale, and lack of requirement for photogrammetry expertise |
| Environmental sensing | Thermal imaging, e.g., for gas escape | Wide coverage and hazardous areas |
| Publicity | Public understanding of science, education, media, and marketing | Topicality, immediacy, and engaging imagery providing geographical context without map interpretation |

Tab. 3.2.3: Comparison between total stations and satellite-based techniques (Yuwono & Prasetyo, 2019)

| Total Station | GPS |
|---|---|
| Indirect acquisition of 3D coordinates | Direct acquisition of 3D coordinates |
| Both horizontal and vertical accuracies are comparable | The horizontal accuracy is better than the vertical accuracy |
| The accuracy depends on the distance, angle and the used prism | The accuracy depends on the satellite availability, atmospheric effect, satellite geometry, multipath Less precise than total station Satellite dependent |
| More precise than GPS Satellite independent | Visibility is not needed Day or night time data collection |
| Needed inter-visibility between the instrument and the prism | |
| Day time data collection | |



Fig. 3.2.2: Unmanned Aerial Vehicle (UAV) with camera (left) and GPS antenna with controller (Leica and Trimble, right, company material)
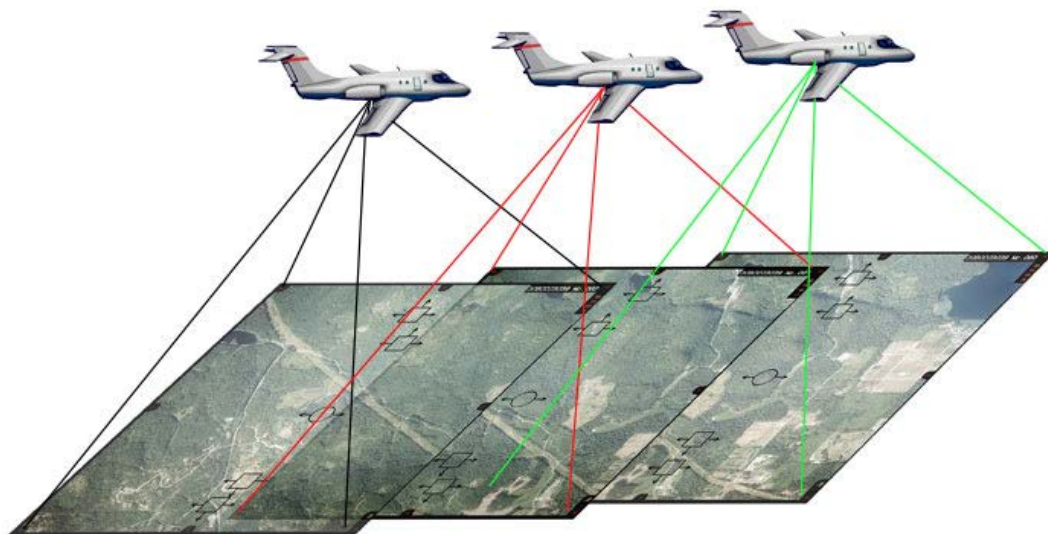


Fig. 3.2.3: Principle of aerial photogrammetry

Surveying for geotechnical engineers

Only for private and internal use!                                Updated: 05 March 2021

## 3.3  Terrestrial laser scanning

Terrestrial laser scanning (TLS) is a modern terrain mapping and monitoring method. TLS measurements are performed from many positions connected with a common reference point. The obtained point cloud provides an image of the scanned space. Typical distances are a few meters of up to a few kilometres. Laser scanning is typically used in one of the following two forms:

- TOF (time-of-flight) measurements (measures travel time of short impulses emitted from the device)

- Phase-shift measurement (continuous beam is transmitted and phase shift between emitted and received signal is evaluated)

Besides these two basic techniques photogrammetric scanning can be performed to obtain the 3D structure of small objects.
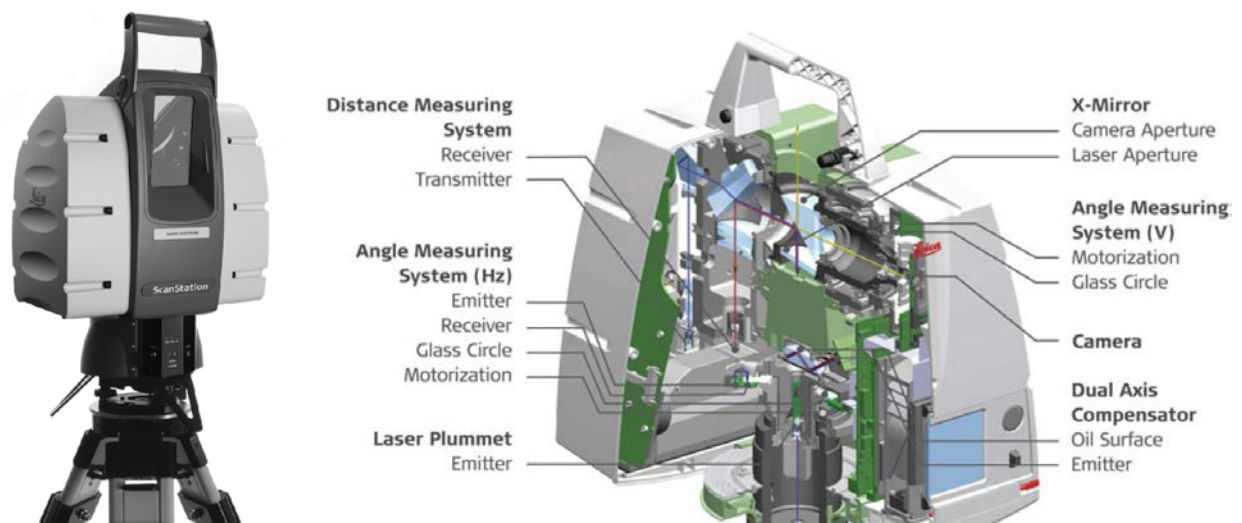


Fig. 3.3.1: Terrestrial laser scanner (Leica geosystems, company material)

TLS is used for many purposes in geoengineering, for instance for:

- Monitoring of landslides / slope stability and deformation

- Observation / monitoring of infrastructure projects like dams, bridges, buildings, tunnels, roads etc.

- Mine slope deformation and stability

- 3D visualisation of archaeological sites

Surveying for geotechnical engineers

Only for private and internal use!          Updated: 05 March 2021

# 4 Accuracy and precision of surveying techniques

Accuracy is the degree of conformity of a given measurement with a standard value. Precision is the extent to which a given set of measurements agree with their mean. Errors are the difference between a measured value and its true value. The true value of a measurement is determined by taking the mean value of a series of repeated measurements. Errors can be subdivided into instrument errors, human errors and natural errors. The aim should be, to reduce the errors to a minimum. This can be reached by precise and careful handling of the instrument, avoiding any kind of operation mistake using the equipment and correction for environmental impacts.

Any survey results should contain a detailed error analysis. Ogundare (2016) and Ghilani & Wolf (2012) explain in detail the corresponding procedures. The following tables provide an impression about accuracy and precision, respectively, in combination with typical ranges of application for different surveying techniques.

Tab. 3.1: Typical range of application and accuracy of different surveying methods (Gili et al., 2000)

| Method/technique | Results | Typical range | Typical precision |
|---|---|---|---|
| Precision tape | distance change | <30 m | 0.5 mm/30 m |
| Fixed wire extensometer | distance change | <10–80 m | 0.3 mm/30 m |
| Rod for crack opening | distance change | <5 m | 0.5 mm |
| Offsets from baseline | coordinates differences (2D) | <100 m | 0.5–3 mm |
| Triangulation | coordinates differences (2D) | <300–1000 m | 5–10 mm |
| Traverse/polygon | coordinates differences (2D) | variable, usually <100 m | 5–10 mm |
| Leveling | height change | variable, usually <100 m | 2–5 mm/km |
| Precise leveling | height change | variable, usually <50 m | 0.2–1 mm/km |
| EDM (Electronic Distance Measurement) | distance change | variable, usually 1–14 km | 1–5 mm + 1–5 ppm |
| Terrestrial photogrammetry | coordinates differences (3D) | ideally <100 m | 20 mm from 100 m |
| Aerial photogrammetry | coordinates differences (3D) | H flight <500 m | 10 cm |
| Clinometer | angle change | $\pm 10^0$ | $\pm 0.01$–$0.1^0$ |
| Precision theodolite | angle change | variable | $\pm 10$ |
| GPS survey | coordinates differences (3D) | variable | 2–5 mm + 1–2 ppm |

Note: 1 ppm means one part per million or 1 additional millimetre per kilometre of measured line.

Tab. 3.2: Resolution quality of airborne photogrammetry (Wyoming, 2013)

| Project Type | Flight Height (ft) | Pixel Resolution (in/pixel) | Ground Coverage Along Flight Line | |
|---|---|---|---|---|
| | | | Length (ft) | Width (ft) |
| Urban Projects (plains) | 1250 | 1.50 | 960 | 1728 |
| Urban Projects (mountainous terrain) | 1500 | 1.80 | 1152 | 2074 |
| Suburban Projects | 1800 | 2.16 | 1382 | 2488 |
| Rural Projects (plains) | 2000 | 2.40 | 1536 | 2765 |
| Rural Projects (mountainous terrain) | 2400 | 2.88 | 1843 | 3317 |
| Systems | 7075 | 8.49 | 5433 | 9779 |
| High altitude city planning imagery | 9500 | 11.40 | 7295 | 13131 |

Tab. 3.3: Accuracy of total station and GPS based measurements (Wyoming, 2013)

| Instrument | Horizontal Accuracy | Vertical Accuracy |
|---|---|---|
| GPS/RTK | 0.034 ft (0.010 m) | 0.066 ft (0.020 m) |
| Optical Total Station | 0.011 ft (0.003 m) | 0.007 ft (0.002 m) |
| Digital Level | N/A | 0.001 ft |

Tab. 3.4: Precision of levelling (Ogundare, 2016)

| Make | Description | Accuracy (Per 1 km Double Run) |
|---|---|---|
| Wild N3 Precision Level | M = 42×; bubble sensitivity/div: 10″; accuracy of leveling line of sight: 0.25″ | ±0.2 mm |
| Leica NA2/NAK2 | Automatic optical levels Magnification: 32× | 0.7 mm (0.3 mm with parallel-plate micrometer); compensator setting accuracy of 0.3″ |
| Leica DNA03 | Digital level Magnification: 24× | 1.0 mm (0.3 mm with invar) |
| Sokkia PL1 | Tilting level Magnification: 42× | 0.2 mm (0.1 mm with micrometer) |
| Sokkia SDL30 | Digital level Magnification: 32× | 1 mm (0.6 mm with invar) |
| Sokkia B20 | Automatic level Magnification: 32× | 1.0 mm (0.8 mm with micrometer) |
| Topcon DL-101C | Digital level Magnification: 32× | 0.4 mm with invar; compensator setting accuracy of 0.3″ |

Tab. 3.5: Precision of distance measuring (Ogundare, 2016)

| Make | Description | Angular/Direction Accuracy | Distance Accuracy |
|------|-------------|---------------------------|-------------------|
| Kern DM502 | Precision EDMs | N/A | Range: 2 km for DM502 and 5 km for DM503 $3\ mm \pm 2.0\ ppm$ |
| Kern ME3000 | Precision EDM | N/A | Range: 2.5 km $0.2\ mm \pm 1.0\ ppm$ |
| Kern ME5000 | Precision EDM | N/A | Range: 8 km $0.2\ mm \pm 0.2\ ppm$ |
| ComRad Geomensor 204DME | Precision EDM | N/A | Range: 10 km $0.1\ mm \pm 0.1\ ppm$ |
| Leica TC2003/ TCA2003 and TC2002 | Without/with ATR total station Magnification: 30× | 0.5″ Resolution: 0.1″ | Range: 2.5/3.5 km $1\ mm \pm 1.0\ ppm$ (with one prism and average weather) |
| Leica TDM/ TDA 5005 | Industrial total station Magnification: 30× | 0.5″ Resolution: 0.1″ | Range: 2–600 m $1\ mm \pm 2.0\ ppm$ |
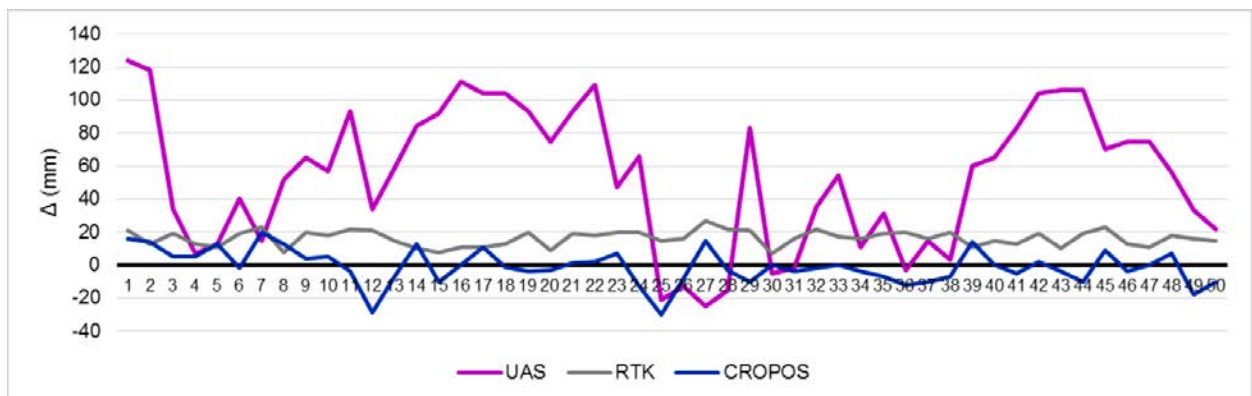


Fig. 3.1:  Deviation (elevation of points) from high precision total station measurements: RTK and CROPOS are satellite-based methods; UAS is an unmanned aerial drone photogrammetric system (Moser et al., 2016)

Tab. 3.6: Accuracy of different LiDAR sensors used in UAVs (Gordian et al. 2020)

|  | LEDDAR TECH VU8 | VELODYNE HDL-32E | RIEGL VUX-1UAV | ROUTESCENE LIDARPOD | YELLOWSCAN SURVEYOR | GEODETICS GEO-MMS |
|---|---|---|---|---|---|---|
| Wavelength (nm) | 905 | 903 | 905 | 905 | 905 | 905 |
| Maximum range (m) | 185 | 100 | 920 | 100 | 100 | 200 |
| Accuracy (cm) | 5 | 2 | 1 | 2 | 5 | 3 |
| Field of view (°) | 100 | 360 | 330 | 360 | 360 | |
| Weight (kg) | 1.3 | 1.3 | 3.5 | 2.5 | 1.5 | 1.5 |

Tab. 3.7: Accuracy and application range of laser scanning (Opitz, 2013)

| Scanner Type | Primary Applications | Typical Accuracy | Typical Range |
|---|---|---|---|
| Triangulation scanner | Object scanning | Less than 1 mm | 0.1 to 1 m |
| Terrestrial TOF Scanner | Architectural scanning | 3–6 mm | 0.5 to 100 m |
| Terrestrial Phase based scanner | Architectural scanning | 5 mm | 0.5 to 100 m |
| Airborne Scanner (light aircraft) | Landscape mapping | 15 cm vertical 50 cm planimetric | 1000 to 3500 m |
| Airborne Scanner (helicopter) | Corridor mapping | 8 cm vertical 20 cm planimetric | 50 to 250 m |
| Mobile Mapping | Urban modelling, coastal erosion monitoring | 10–50 mm | 100–200 m |

Tab. 3.8: Accuracy of TLS (Soudarissanane, 2016)

| Manufacturer | Model | Type | Max. Range | Single point accuracy | Max. Scan rate (pts/sec) |
|---|---|---|---|---|---|
| FARO | Focus 3D | Phase | 0.6m - 120m | ±2mm | 976 000 |
| Leica | P-20 | Pulse/WFD [1] | 0.1m - 120m | ±3mm | 1 000 000 |
| Leica | HDS-7000 | Phase | 0.3m - 187m | ±1.2mm | 1 016 727 |
| Leica | C-10 | Pulse | 0.1m - 300m | ±6mm | 50 000 |
| Topcon | GLS-1500 | Pulse | 1m - 330m | ±4mm | 30 000 |
| Riegl | VZ-6000 | Pulse | 5m - 6000m | ±15mm | 37 000 |

Surveying for geotechnical engineers

Only for private and internal use!                                    Updated: 05 March 2021

# 5   Rock mechanical examples

## 5.1   DEM for a rock mass system

Herbst & Konietzky (2012) describe the use of 3D numerical modelling to investigate potential rockfall in a sandstone massif (Fig. 5.1.1). The workflow illustrated in Fig. 5.1.2 starting with in-situ investigations and measurements and ending with a stability analysis based on a numerical model. The numerical model is based on a DEM obtained by terrestrial laser scanning with resolution of 5 cm, which corresponds to 11.5 Mio points (Fig. 5.1.3) supplemented by airborne photogrammetry. Fig. 5.1.4 shows a plane view of the DEM after smoothing and filtering procedure. Exemplary, Fig. 5.1.5 shows a simulation result of the numerical model.
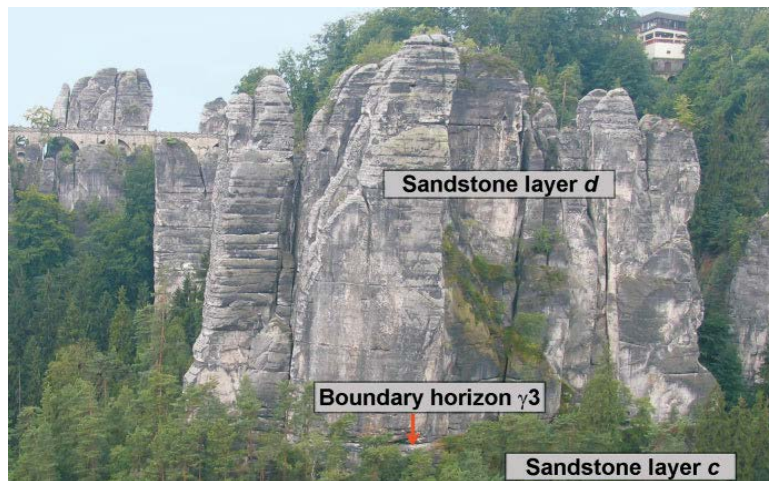


Fig. 5.1.1: Photo of sandstone massive under investigation (Herbst & Konietzky, 2012)
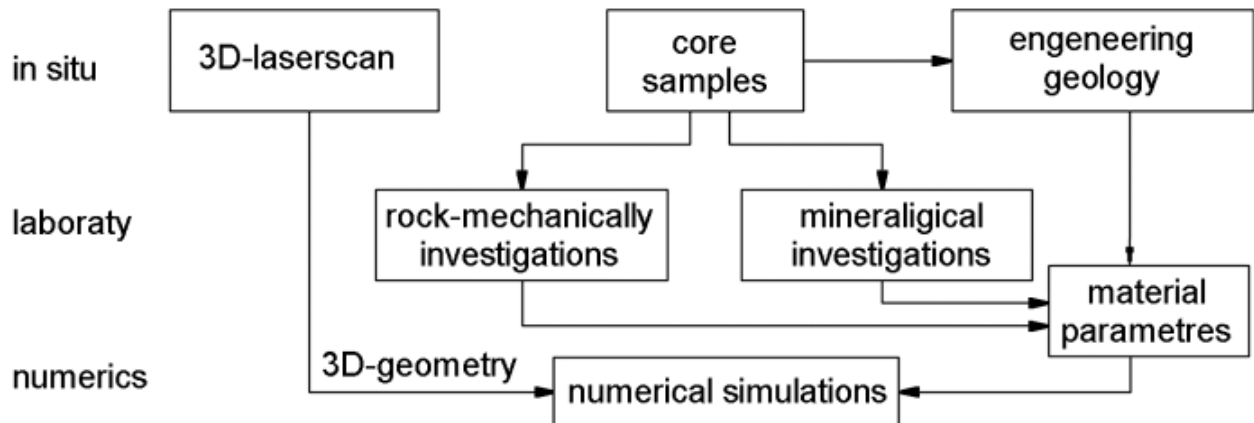


Fig. 5.1.2: General workflow scheme (Herbst & Konietzky, 2012)
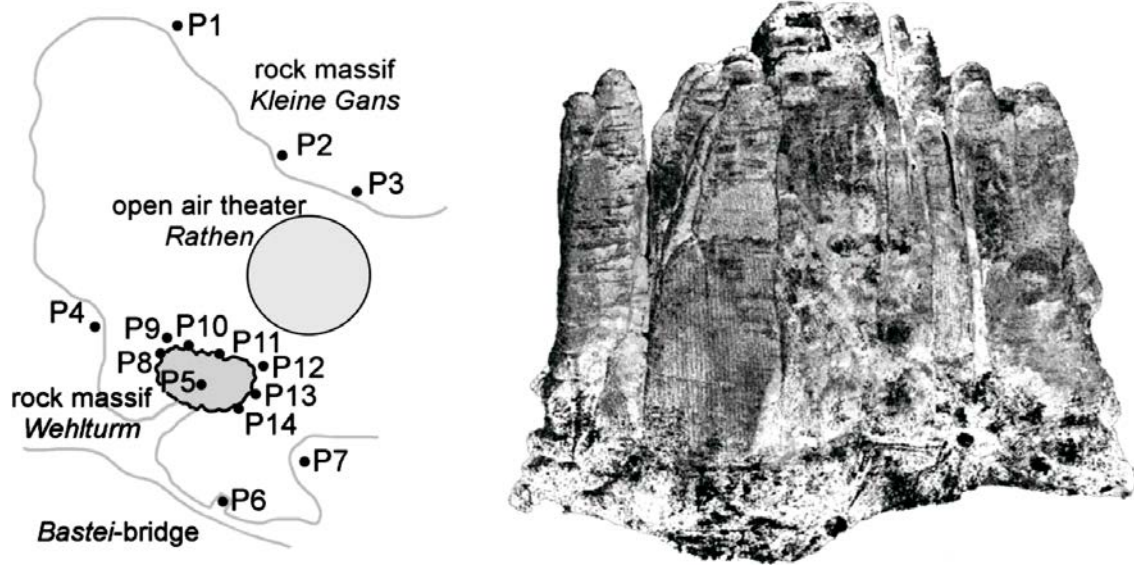
Fig. 5.1.3: Position of TLS devices (left) and point cloud as TLS result (right; both: Herbst & Konietzky, 2012)
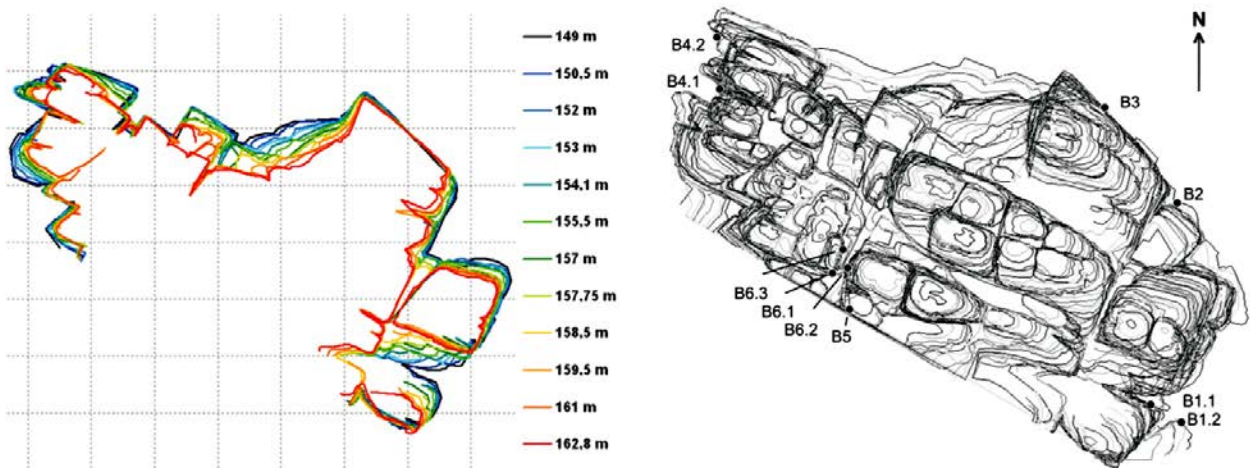


Fig. 5.1.4: Plane view of TLS results after data management (Herbst & Konietzky, 2012)
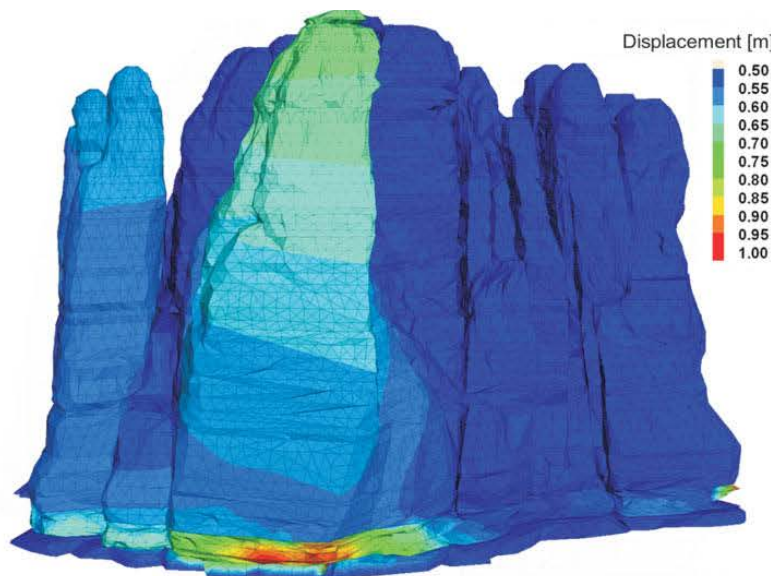


Fig. 5.1.5: Simulation result of the numerical model based on TLS data (Herbst & Konietzky, 2012)

Surveying for geotechnical engineers

Only for private and internal use!                                                                Updated: 05 March 2021

## 5.2  *Surface movements due to mining activity*

During active mining, but also during flooding of mines significant surface movements take place. Numerical simulation can help to predict such movements and to understand the mechanisms behind. The following example is related to the abandoned coal mine region Lugau-Oelsnitz in Germany (Lüttschwager et al., 2020; Zhao & Konietzky, 2020). Survey data are used for the calibration of the numerical model, so that prediction becomes reliable. Fig. 5.2.1 shows the annual surface uplift rates for different time periods obtained from ground-based levelling and satellite data (InSAR). Fig. 5.2.2 shows a comparison between survey data and numerical model results and Fig. 5.2.3 shows numerical predictions for surface movement in the future up to the year 2038. The general numerical simulation procedure is documented in Fig. 5.2.4. This project is a good example to document the combined use of total station and InSAR measurements. The first one has higher accuracy, but is restricted to several points; the latter is less precise, but delivers data for a large area. Also, InSAR data are always available, specific measurement campaigns like for total station measurements are not necessary.
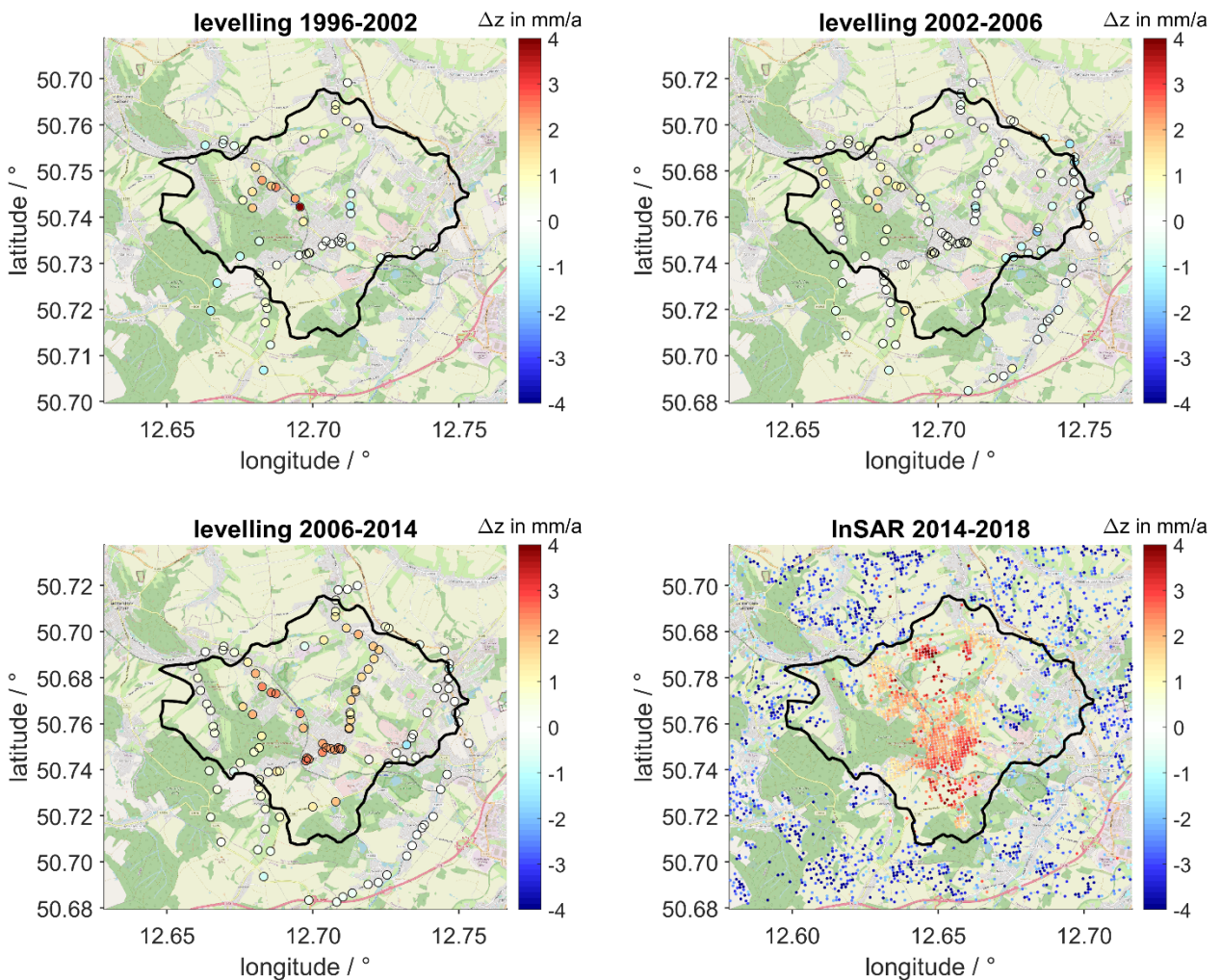


Fig. 5.2.1: Annual surface uplift rates for different time periods based on ground levelling and InSAR data, the thick black line marks the envelope of the mining area (Lüttschwager et al., 2020).
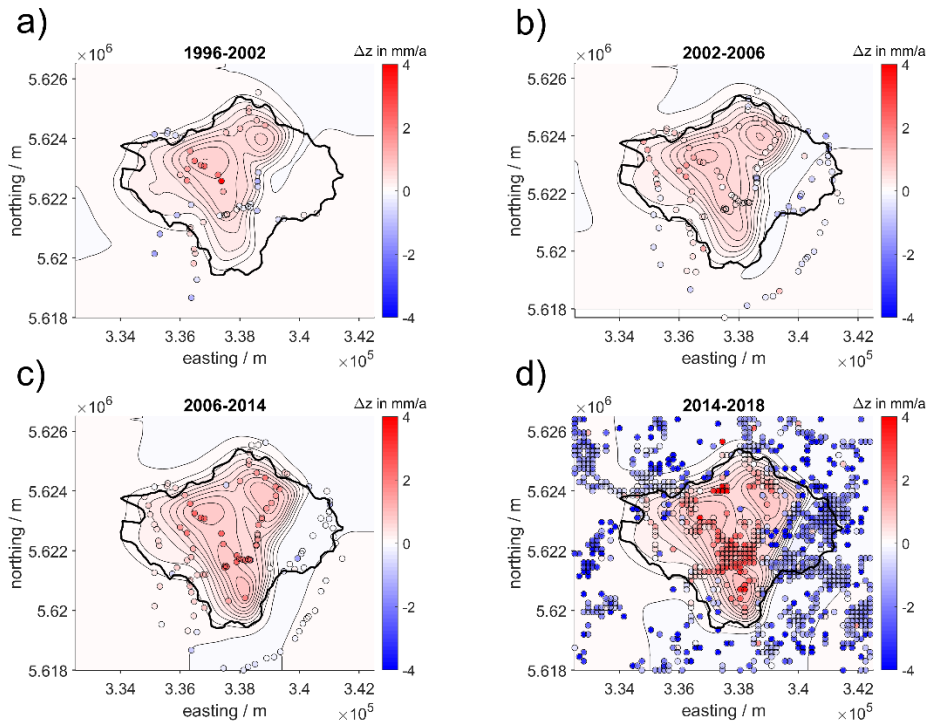
Surveying for geotechnical engineers

Only for private and internal use!                                    Updated: 05 March 2021

Fig. 5.2.2: Numerical modelling results for vertical uplift compared with levelling and InSAR data (Lüttschwager et al., 2020)
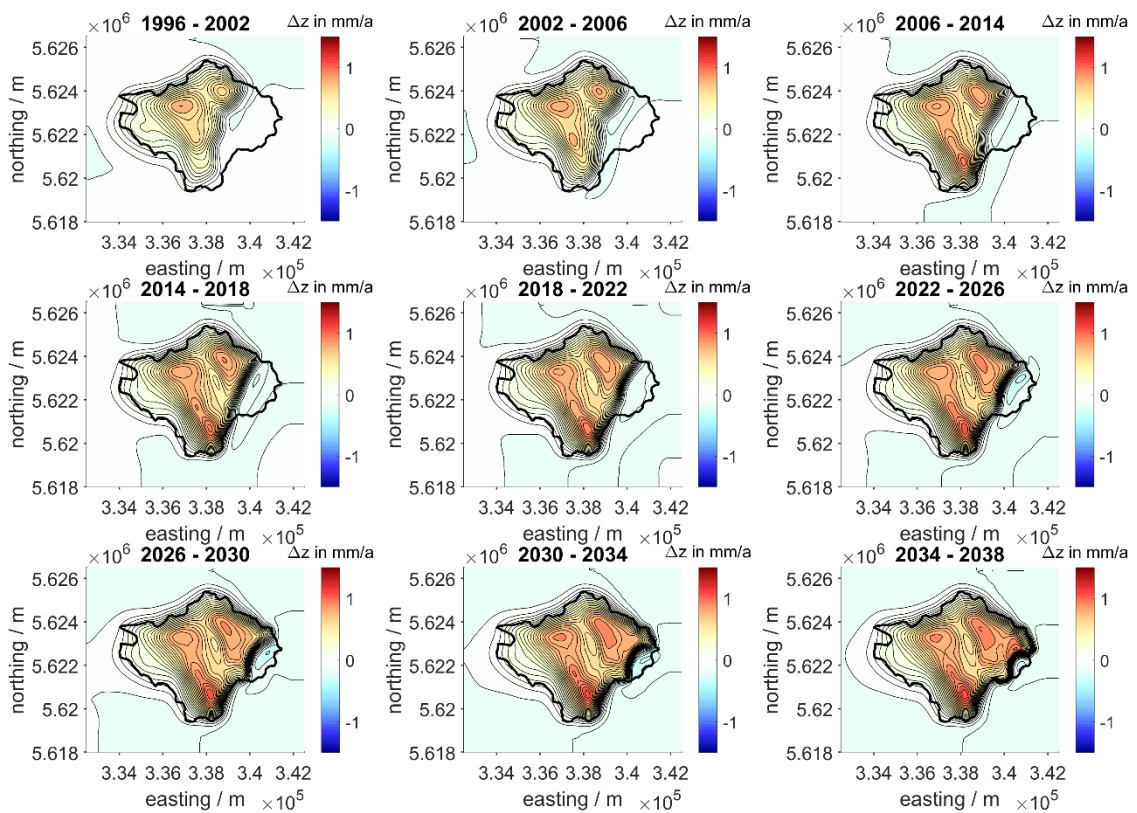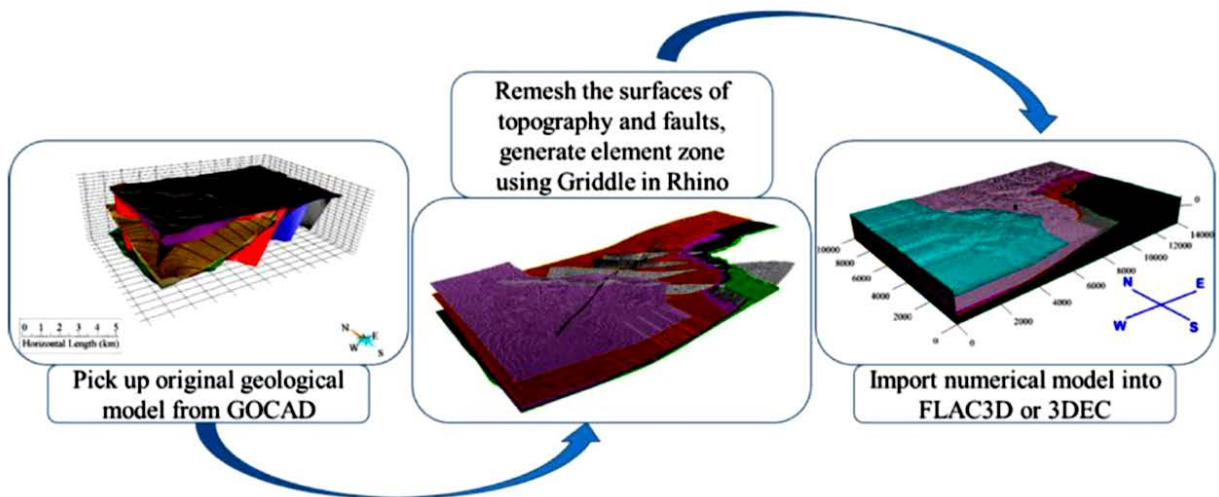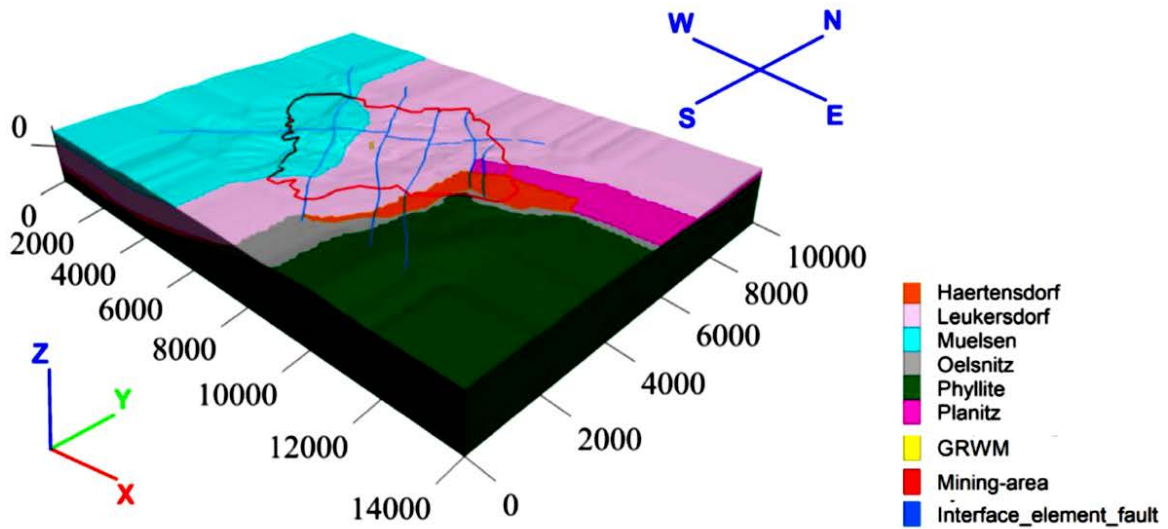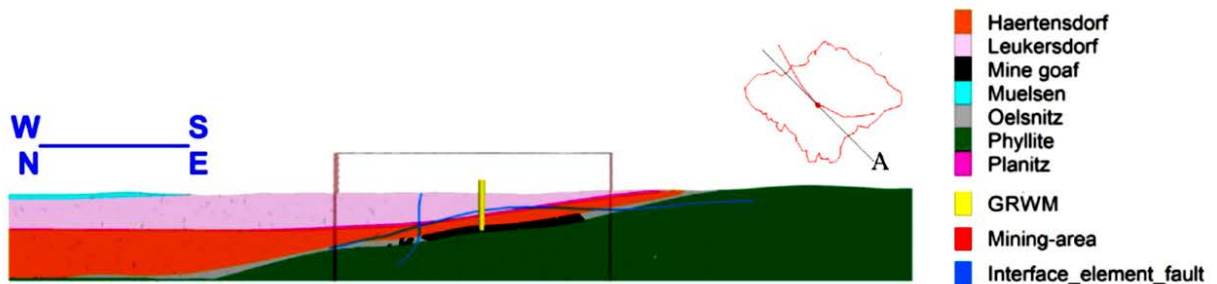


Fig. 5.2.3: Numerical modelling results for vertical uplift (Lüttschwager et al., 2020)

(a) Illustration of modeling procedure (from geological model to numerical model)



(b) Oelsnitz numerical model [m]



(c) Approximate cross section A

Fig. 5.2.4: Workflow of numerical modelling procedure to predict uplift (Zhao & Konietzky, 2020)

Surveying for geotechnical engineers

Only for private and internal use!                                    Updated: 05 March 2021

## 5.3 Deformation survey for water dams

Water dams are critical infrastructure elements which need careful monitoring to avoid any damage which could lead to disasters. Besides geotechnical measurements like extensometer, inclinometer, Fissurometer, load cell, piezometer etc. measurements, also geodetic surveying plays an important role. Dam surveying goes down to the sub-millimetre range and depending on type of measurement they are performed frequently (either continuously or daily or weekly) or in longer time intervals (monthly, yearly). Survey data are input for any kind of geotechnical stability and deformation analysis mainly performed via numerical modelling. Typical surveying methods for dam monitoring are (e.g. Scaioni & Wang, 2016; Scaioni, 2018):

- Terrestrial laser scanning
- Ground-based and spaceborne InSAR
- Digital photogrammetry
- Total station measurements / optical levelling

Berberan et al. (2011) document the combined usage of TLS and photogrammetry to monitor dam deformations. For TLS 3 scan positions and 27 reflectors were used (Fig. 5.3.1). Deformations deduced from TLS are documented in Fig. 5.3.2 and 5.3.3.
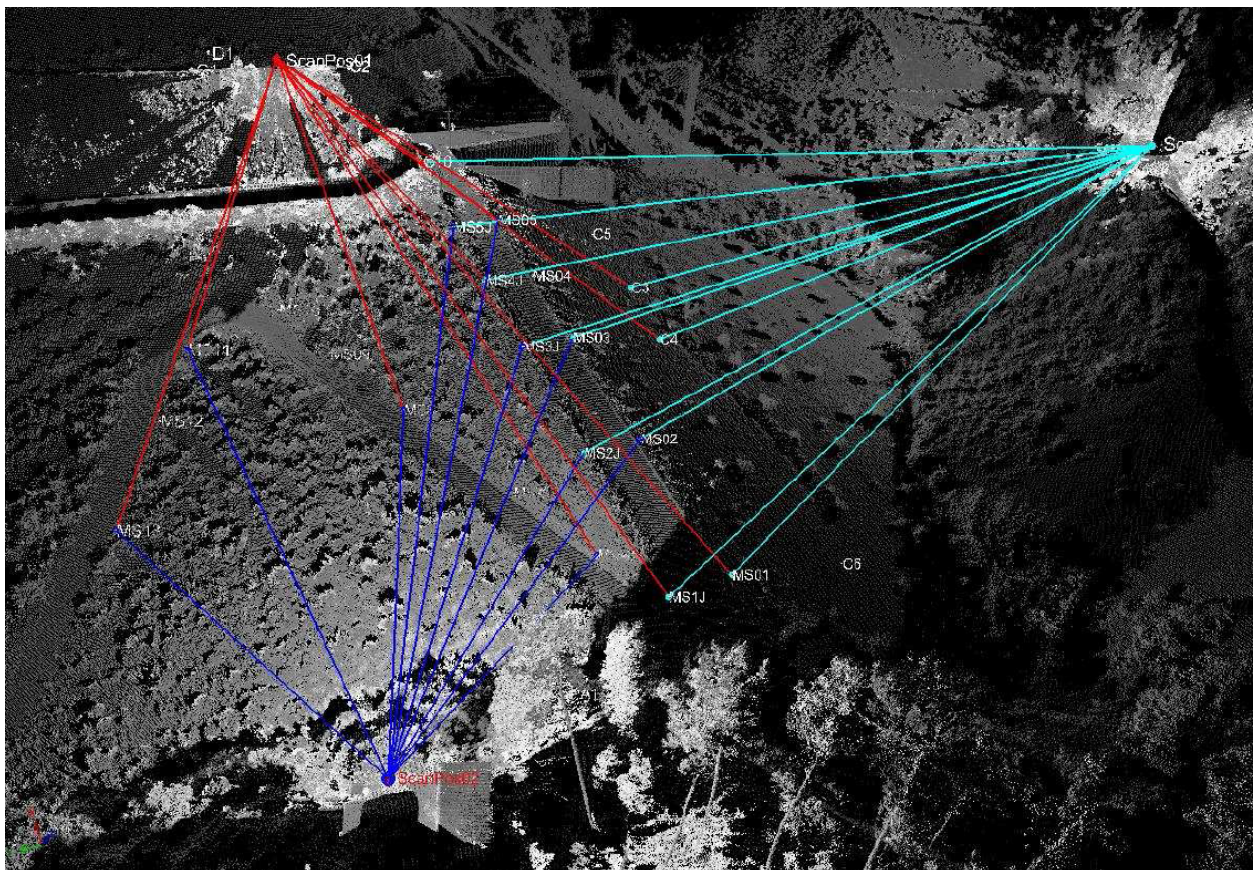


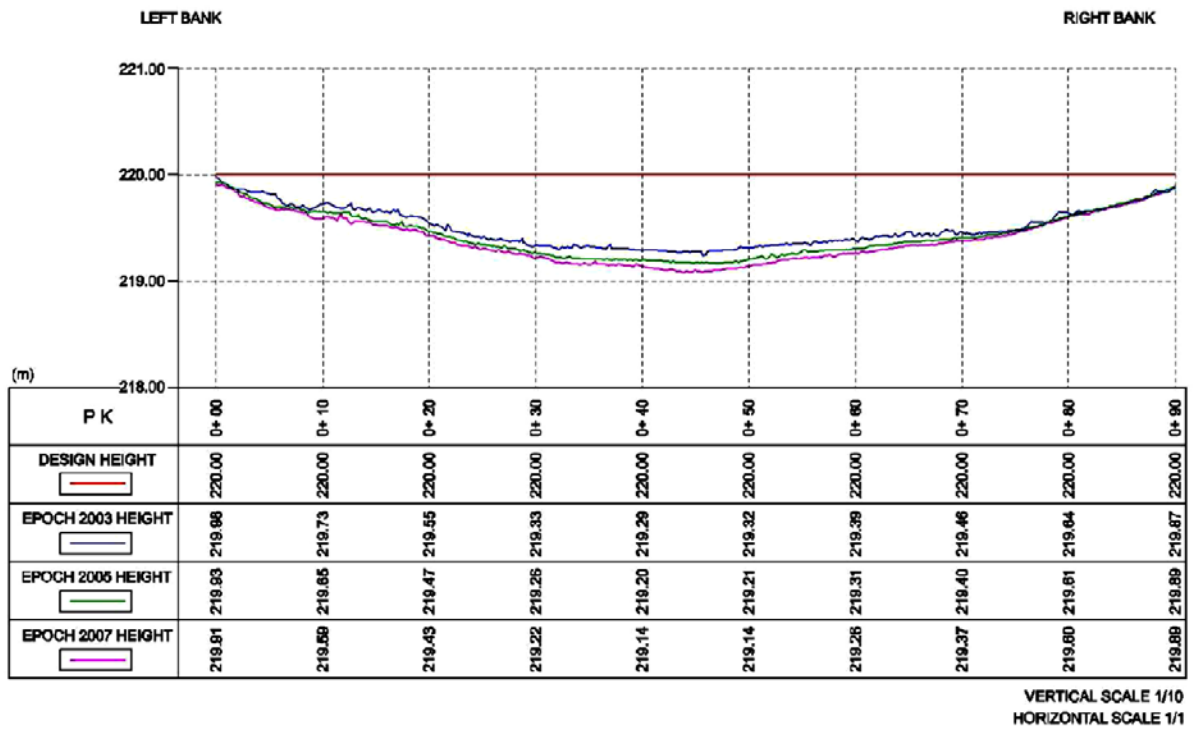Fig. 5.3.1: Point cloud obtained from TLS including scan and reflector positions (Berberan et al., 2011)

| LEFT BANK | | | | | | | | | RIGHT BANK |

| P K | 0+00 | 0+10 | 0+20 | 0+30 | 0+40 | 0+50 | 0+60 | 0+70 | 0+80 | 0+90 |
|---|---|---|---|---|---|---|---|---|---|---|
| DESIGN HEIGHT | 220.00 | 220.00 | 220.00 | 220.00 | 220.00 | 220.00 | 220.00 | 220.00 | 220.00 | 220.00 |
| EPOCH 2003 HEIGHT | 219.98 | 219.73 | 219.55 | 219.33 | 219.29 | 219.32 | 219.39 | 219.46 | 219.64 | 219.87 |
| EPOCH 2005 HEIGHT | 219.93 | 219.65 | 219.47 | 219.26 | 219.20 | 219.21 | 219.31 | 219.40 | 219.61 | 219.89 |
| EPOCH 2007 HEIGHT | 219.81 | 219.59 | 219.43 | 219.22 | 219.14 | 219.14 | 219.26 | 219.37 | 219.60 | 219.89 |

VERTICAL SCALE 1/10
HORIZONTAL SCALE 1/1

Fig. 5.3.2: Longitudinal cross section (design surface and real values from 2003, 2005 and 2007) based on TLS data (Berberan et al., 2011)
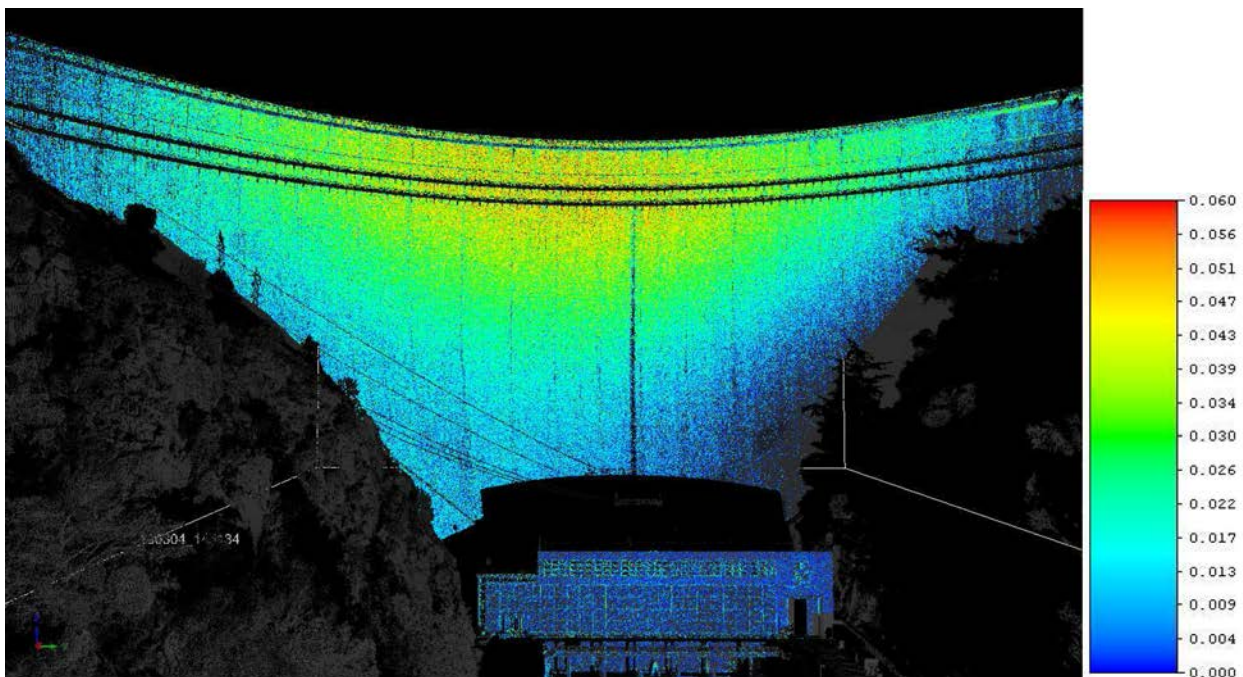


Fig. 5.3.3: Deformation (in m) of the dam between March and August 2010 deduced from TLS (Berberan et al., 2011)

## 5.4   *Landslide surveying*

Landslide surveying can be classified as follows:

- landslide recognition and backanalysis
- monitoring of active landslides

Liu & Wang (2008), Gili et al. (2000) and Scaioni et al. (2014) provide an overview about methods used in landslide surveying (see also Fig. 5.4.1 and 5.4.2). Kovacs et al. (2019) document the monitoring of a landslide via a total station network. Fig. 5.4.3 to 5.4.6 illustrate the obtained results.
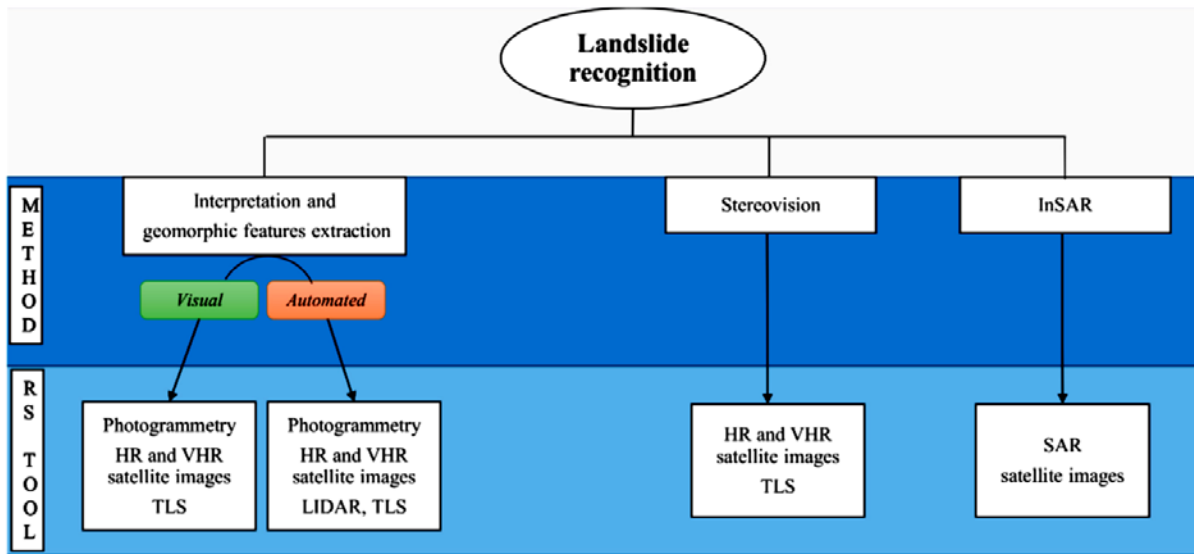


Fig. 5.4.1: Surveying techniques for landslide recognition: HR: High Resolution; VHR: Very High Resolution (Scaioni et al., 2014)
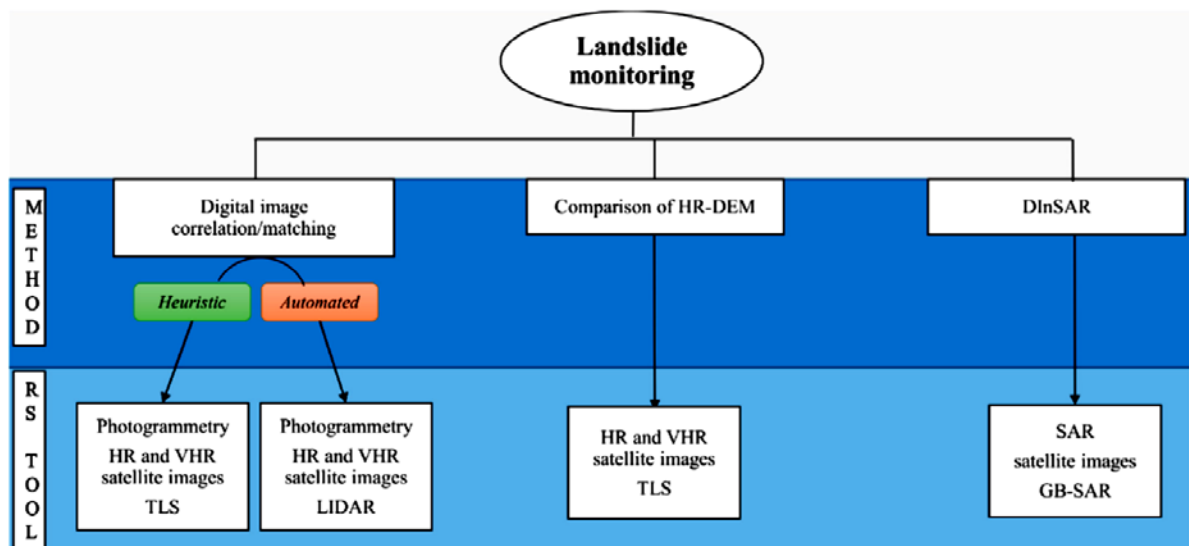


Fig. 5.4.2: Surveying techniques for landslide monitoring: HR: High Resolution; VHR: Very High Resolution (Scaioni et al., 2014)
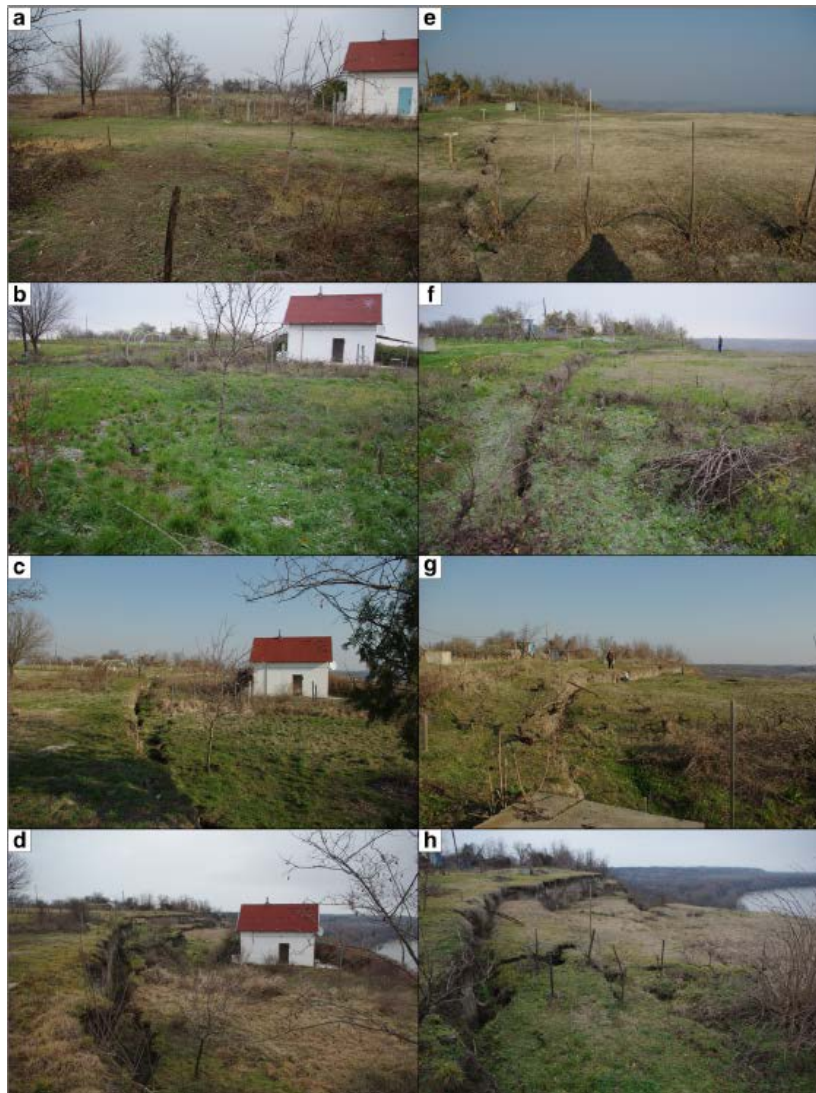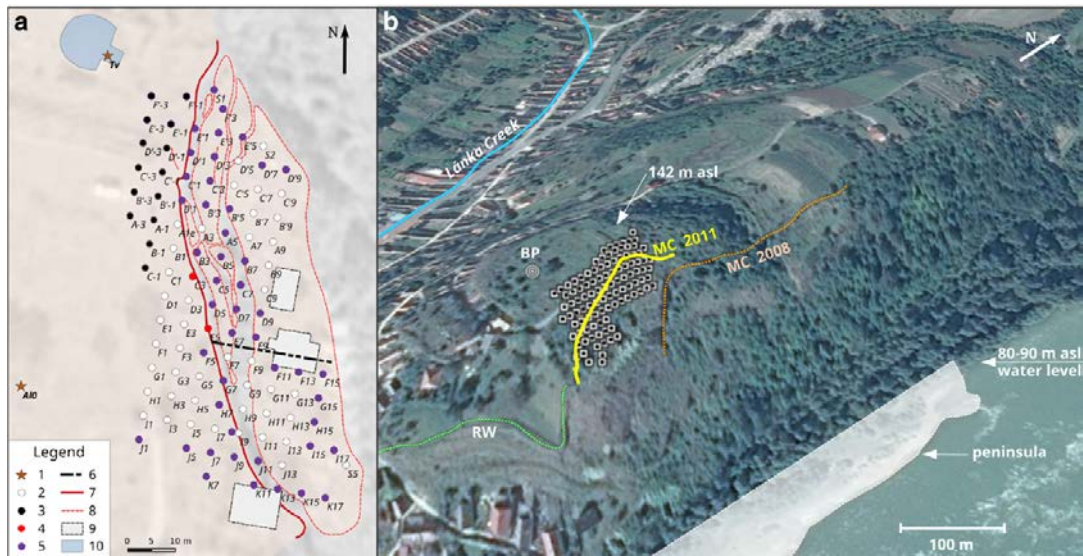
Fig. 5.4.3: Top: landslide location with monitoring points; bottom: photographic documentation of the land-slide evolution with visually recognizable the crack development (Kovacs et al., 2019)
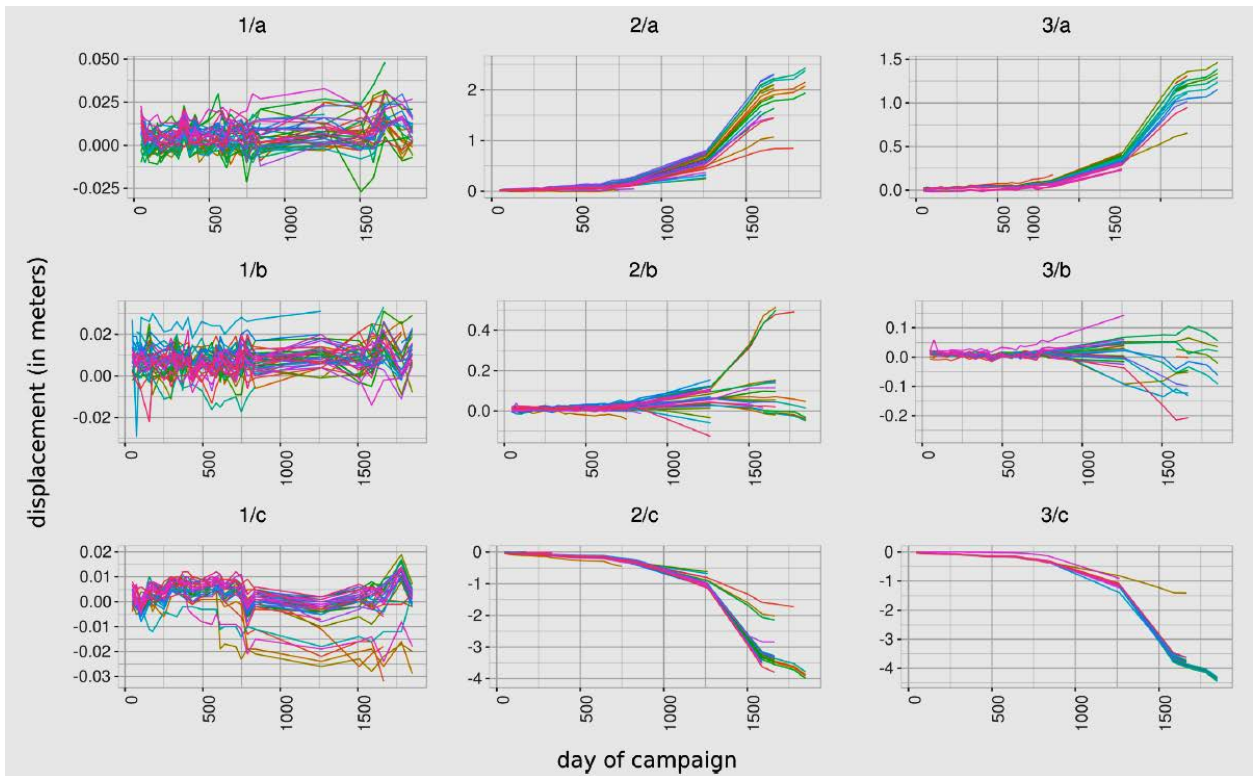
Fig. 5.4.4: Displacements of monitoring points in different regions (1 = x-component, 2 = y-component, 3 = z-component) (Kovacs et al., 2019)
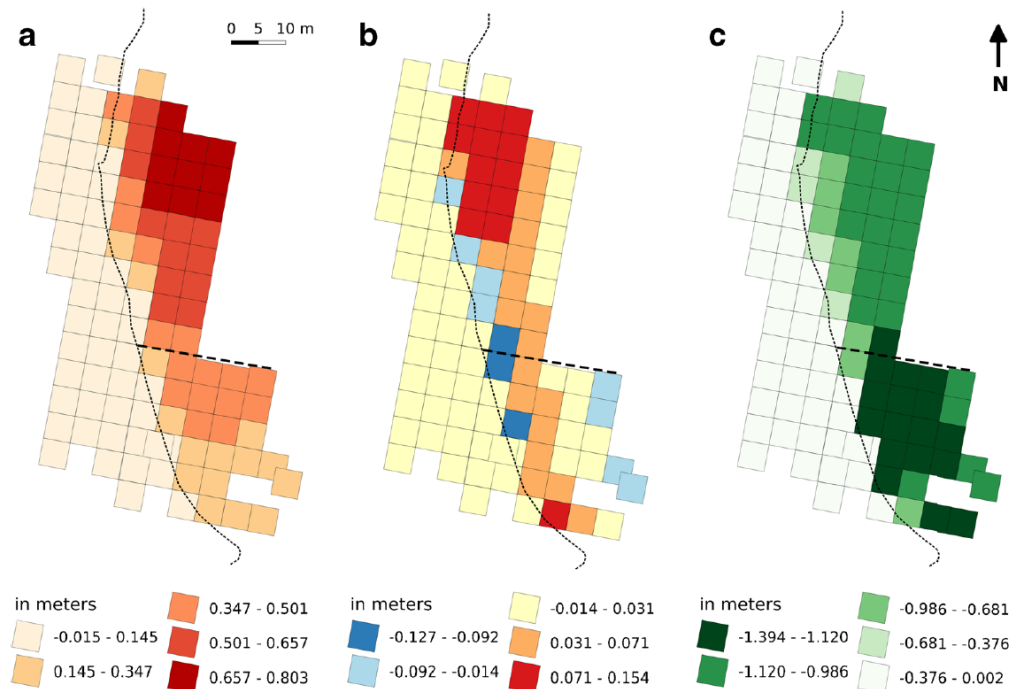


Fig. 5.4.5: Measured displacements during first measuring campaign (a: x-component, b: y-component, c: z-component) (Kovacs et al., 2019)
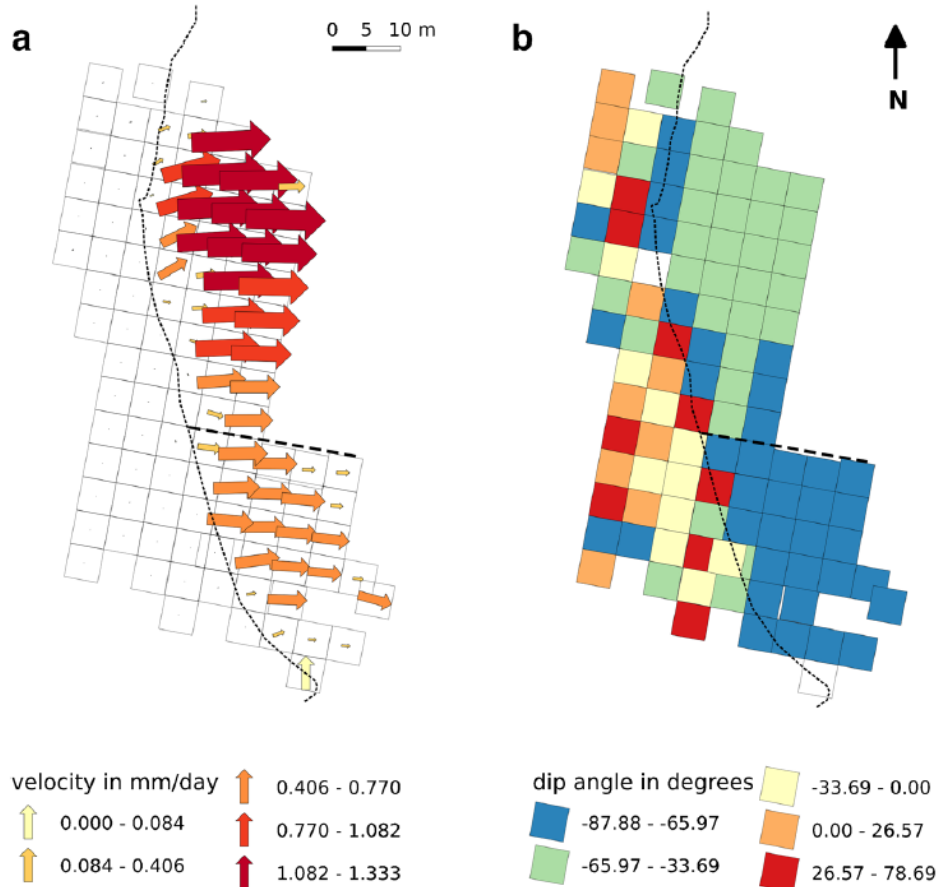
Fig. 5.4.6: Velocities, movement direction and dip angles of measured displacements (Kovacs et al., 2019)

Samsonov et al. (2020) have used differential InSAR (DInSAR) in combination with the multidimensional small baseline subset method (MSBAS-3D) to monitor the Funu landslide in Congo, Africa (see Fig. 5.4.7). The total landslide thickness is about 400 m, while the height of the main scarp is about 100 m. The used pixels have a distance of 5 m x 5 m and the estimated precision is better than 2.8 mm, 1.4 mm and 0.5 mm for north, east and vertical direction, respectively. Fig. 5.4.8 to 5.4.11 show the obtained displacement rates. The movement is very slow in the order of 20 to 50 mm/year. Data from 3/2015 to 1/2019 were evaluated. Based on these high-resolution survey data, geotechnical risk analysis incl. numerical modelling and long-term prediction has to follow.

Surveying for geotechnical engineers

Only for private and internal use!                                          Updated: 05 March 2021



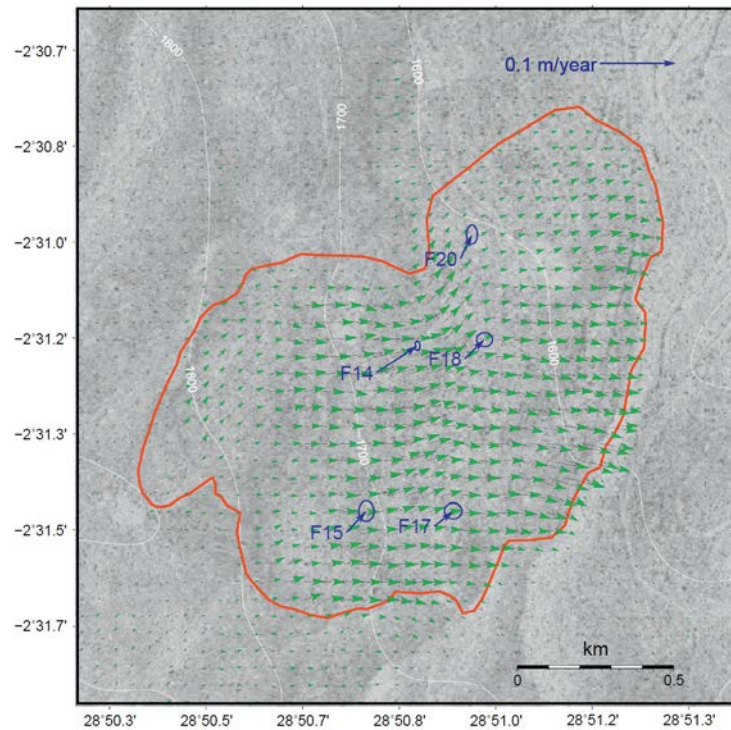Fig. 5.4.7: Drone photograph of Funu landslide (Congo, Africa) (Samsonov et al., 2020)



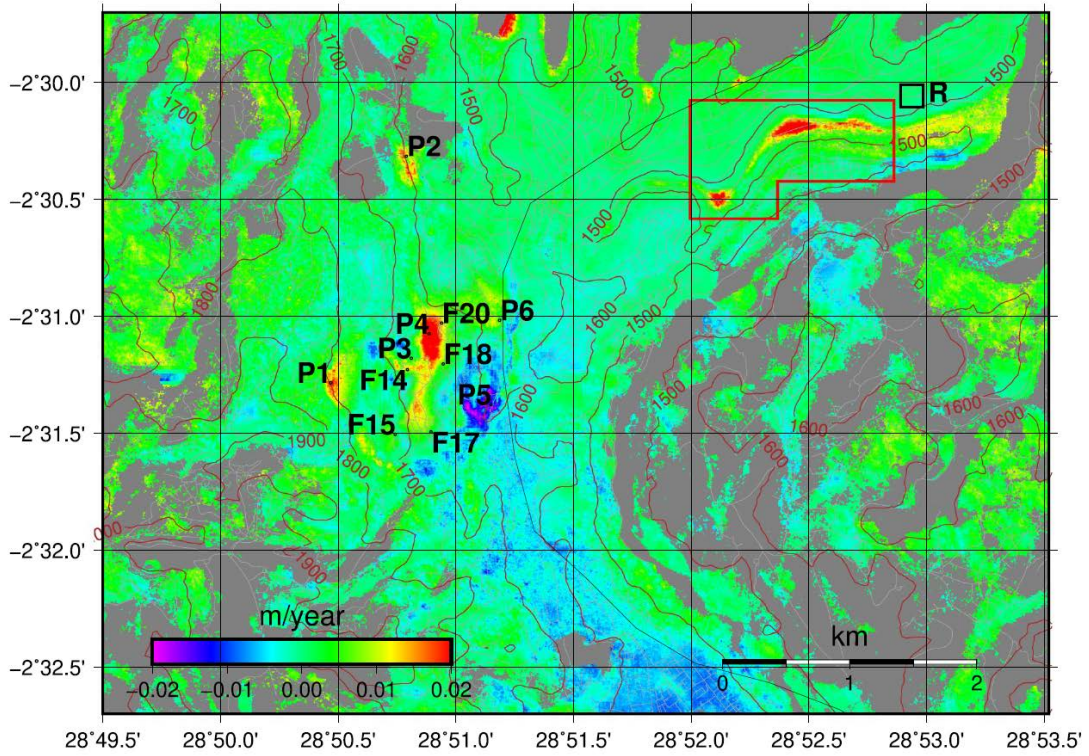Fig. 5.4.8: Deduced horizontal deformation rates (Samsonov et al., 2020)

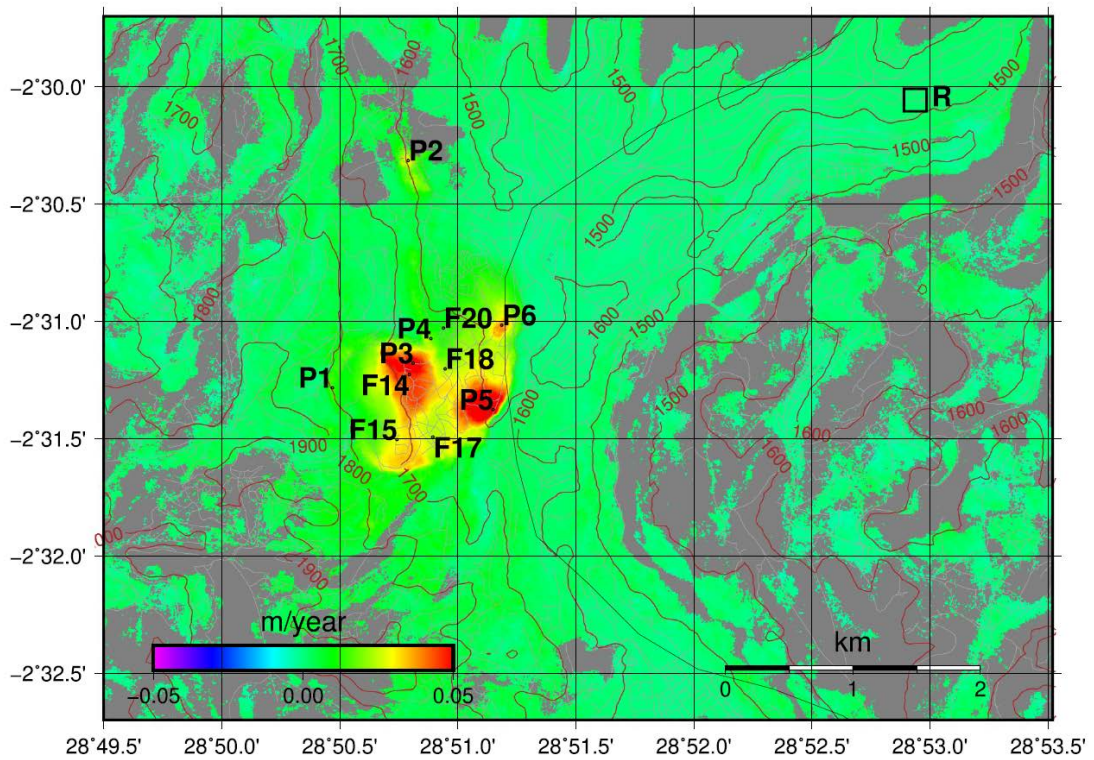Fig. 5.4.9: Northward component of displacement rate (Samsonov et al., 2020)



Fig. 5.4.10: Eastward component of displacement rate (Samsonov et al., 2020)
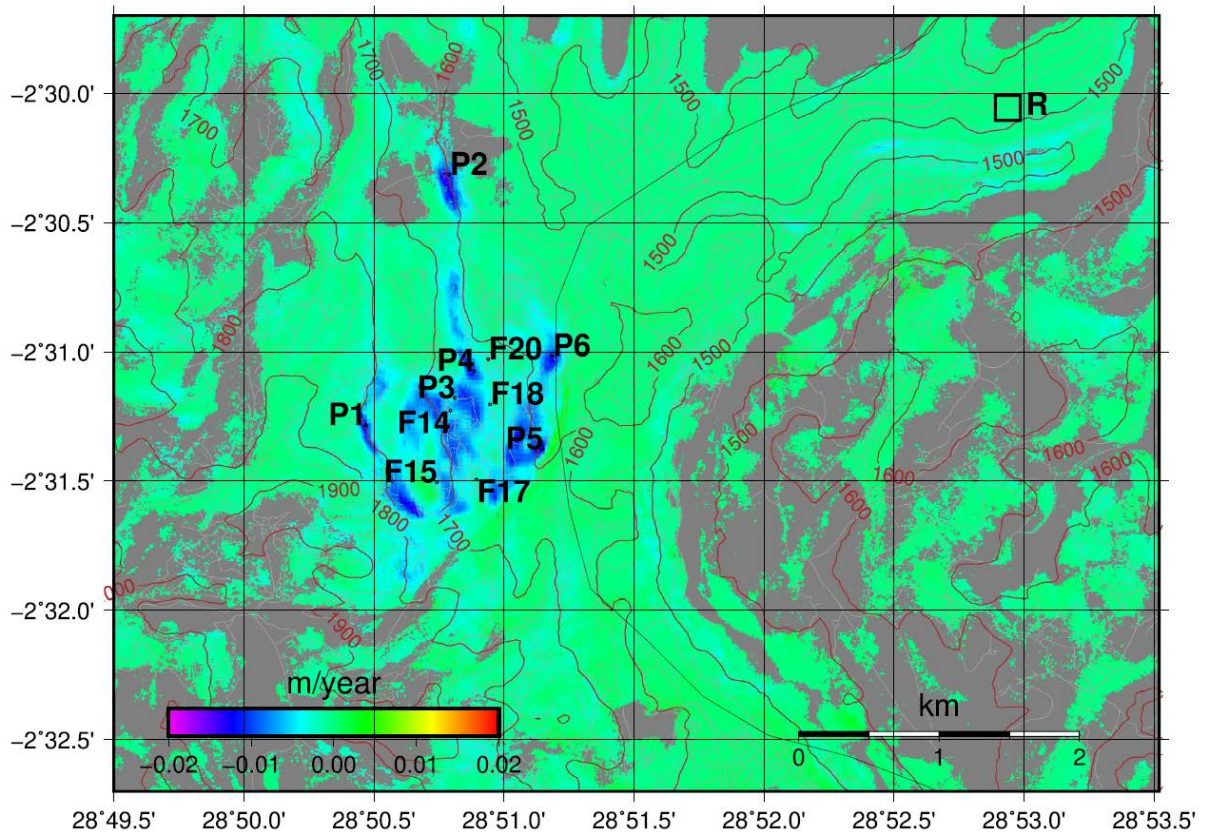
Surveying for geotechnical engineers

Only for private and internal use!                                      Updated: 05 March 2021

Fig. 5.4.11: Vertical component of displacement rate (Samsonov et al., 2020)

## 5.5  *Monitoring of ground movement due to water table drawdown*

Satellite data like InSAR data cannot be used for real-time monitoring, but they can be used to analyse surface movements like settlement or uplift in the past. Data are permanently and globally available since about 1998.

Fig. 5.4.12 shows InSAR monitoring results for an area with water table drawdown. Induced settlement reaches up to 35 mm within about 2 years. Under the assumption of 30 separate recordings for a time period of about 2 years the precision equals ± 5 mm for displacement magnitude and about 1 mm/year for displacement velocity.
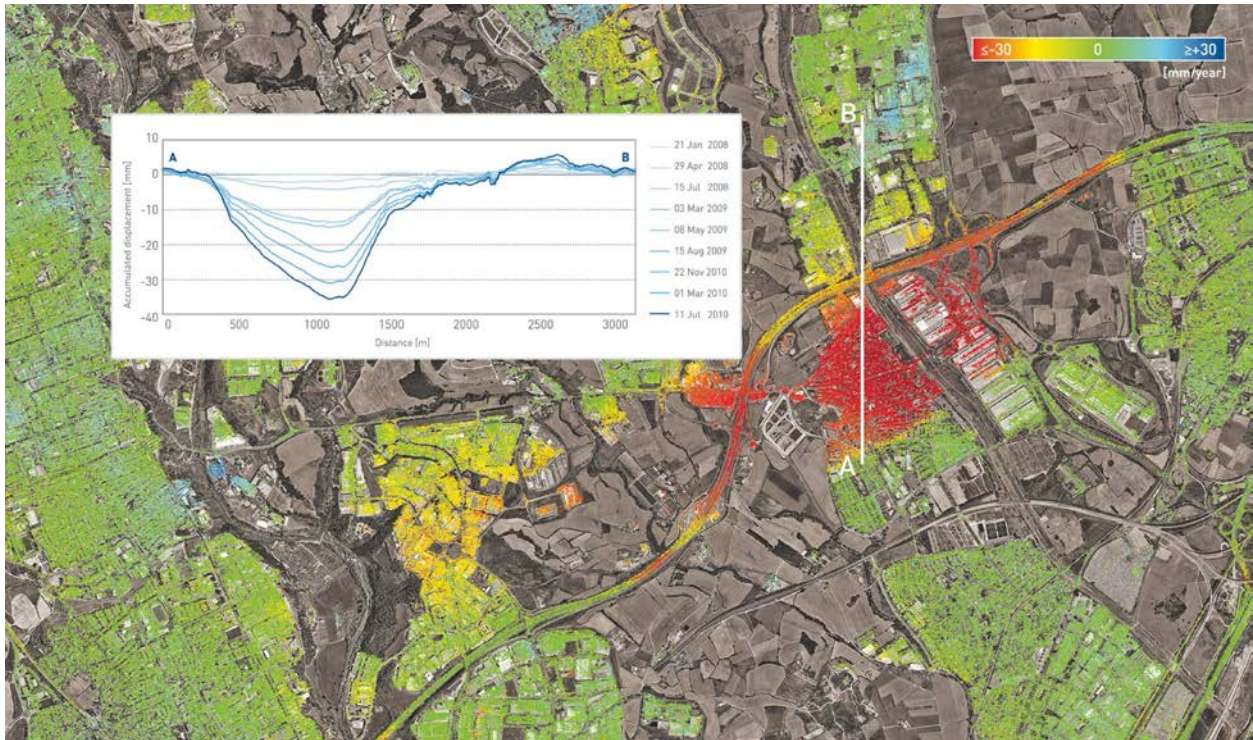
Fig. 5.4.12: InSAR data for monitoring surface movement due to water extraction: contour plot of vertical ground surface movement velocity [mm/year] and vertical displacements [mm] along the profile A-B for several points in time (Radoncic et al., 2021)

Surveying for geotechnical engineers

Only for private and internal use!         Updated: 05 March 2021

# 6   References

Berberan, A.; Ferreira, I.; Portela, E.; Oliveira, S.; Oliveira, A. & Baptista, B. (2011). Overview on terrestrial laser scanning as a tool for dam surveillance, *Proc. 6th Conf. on Dam Engineering*, Lisbon, Portugal, 15.-17. February 2011, 11 p.

EU (2019): Report on surveying user needs and requirements – outcome of the European GNSS' user consultation platform, GSA-MKD-SM-UREQ-229766; Issue/Revision: 2.0

Ghilani, C.D. & Wolf, P.R. (2012): Elementary surveying – an introduction into geomatics, Prantis Hall, 983 p.

Gili, J.A.; Corominas, J. & Rius, J. (2000): Using global positioning system techniques in landslide monitoring, *Engineering Geology*, 55(3): 167-192

Gordian, D. et al. (2020): The use of unmanned aerial vehicles (UHVs) for engineering geology applications, *Bull. of Eng. Geology and the Environment*, 79: 3437-3481

Herbst, M. & Konietzky, H. (2012): Numerical modelling of natural rock formations to estimate stability using the example for a sandstone massif in Saxony, *Geomechanics and Tunneling*, 5(4): 379-388

Kovacs, I.P.; Czigány, S.; Dobre, B.; Fábián, S.Á.; Sobucki, M.; Varga, G. & Bugya, T. (2019): A field survey-based method to characterize landslide development: a case study at the high bluff of the Danube, south-central Hungary, *Landslides*, 16: 1567-1581

Lienhart, W. (2017): Geotechnical monitoring using total stations and laser scanners: critical aspects and solutions, *J. Civil Struct. Health Monitoring*, 7: 315-324

Liu, S.T. & Wang, Z.W. (2008): Choice of surveying methods for landslide monitoring, *Landslides and Slopes*, Taylor & Francis, 1211-1216

Lüttschwager, G.; Zhao, J. & Konietzky, H. (2020): Ground movement predictions above coal mines after flooding, *Proc. 49. Geomechanics Colloquium*, Heft 2020-4: 107-129, Geotechnical Institute, TU Bergakademie Freiberg, Germany

Moser, V.; Barišić, I.; Rajle, D. & Dimter, S. (2016): Comparison of different survey methods data accuracy for road design and construction, *Proc. 4th CETRA conference*, 23.-25. May 2016; 9 p.

Ogundare, J.O. (2016): Precision surveying – The principles and geometrics practice, Wiley, 714 p.

Opitz, R.S. (2013): An overview of airborne and terrestrial laser scanning in archaeology, in: *Interpreting archaeological topography*, Oxbow books, 13-31

Samsonov, S.; Dille, A.; Dewitte, O.; Kervyn; F. & d'Orreye; N. (2020): Satellite interferometry for mapping surface deformation time series in one, two and three dimensions: a new method illustrated on a slow-moving landslide, *Engineering Geology*, 266: 105471

Scaioni, M. & Wang, J. (2016): Technologies for dam deformation measurement: recent trends and future challenges, *Proc. JISDM-2016*, Vienna, 8 p.

Scaioni, M.; Longoni, L.; Melillo, V. & Papini, M. (2014): Remote sensing for landslide investigation: an overview of recent achievements and perspectives, *Remote Sensing*, 6: 9600-9652.

Scaioni, M.; Marsella, M.; Crosetto; M.; Tornatore; V. & Wang; J. (2018): Geodetic and remote-sensing sensors for dam deformation monitoring, *Sensors (Basel)*, 18(11): 3682

Sudarissanane, S.S. (2016): The geometry of terrestrial laser scanning; identification of errors, modeling and mitigation of scanning geometry, doctoral thesis, TU Delft

Wyoming (2013): Survey manual, Wyoming Department of Transportation; http://www.dot.state.wy.us/home/engineering_technical_programs/photos_and_surveys/SurveyManual.html; last accessed: 30.11.2020.

Yuwono, B.D. & Prasetyo, Y. (2019): Analysis deformation monitoring techniques using GNSS survey and terrestrial survey, *Earth and Environmental Science*, 131: 012045

Zhao, J. & Konietzky, H. (2020): Numerical analysis and prediction of ground surface movement induced by coal mining and subsequent groundwater flooding, *Int. Journal of coal Geology*, 229: 103565